Electronic Supplementary Information

Ruthenium, copper and ruthenium-copper complexes of an unsymmetrical phosphino pyridyl 1,8-naphthyridine PNNN ligand

Jingyun Wu, Michael A. Stevens, Michael G. Gardiner, Annie L. Colebatch

Contents

1. Characterisation data for PNNN

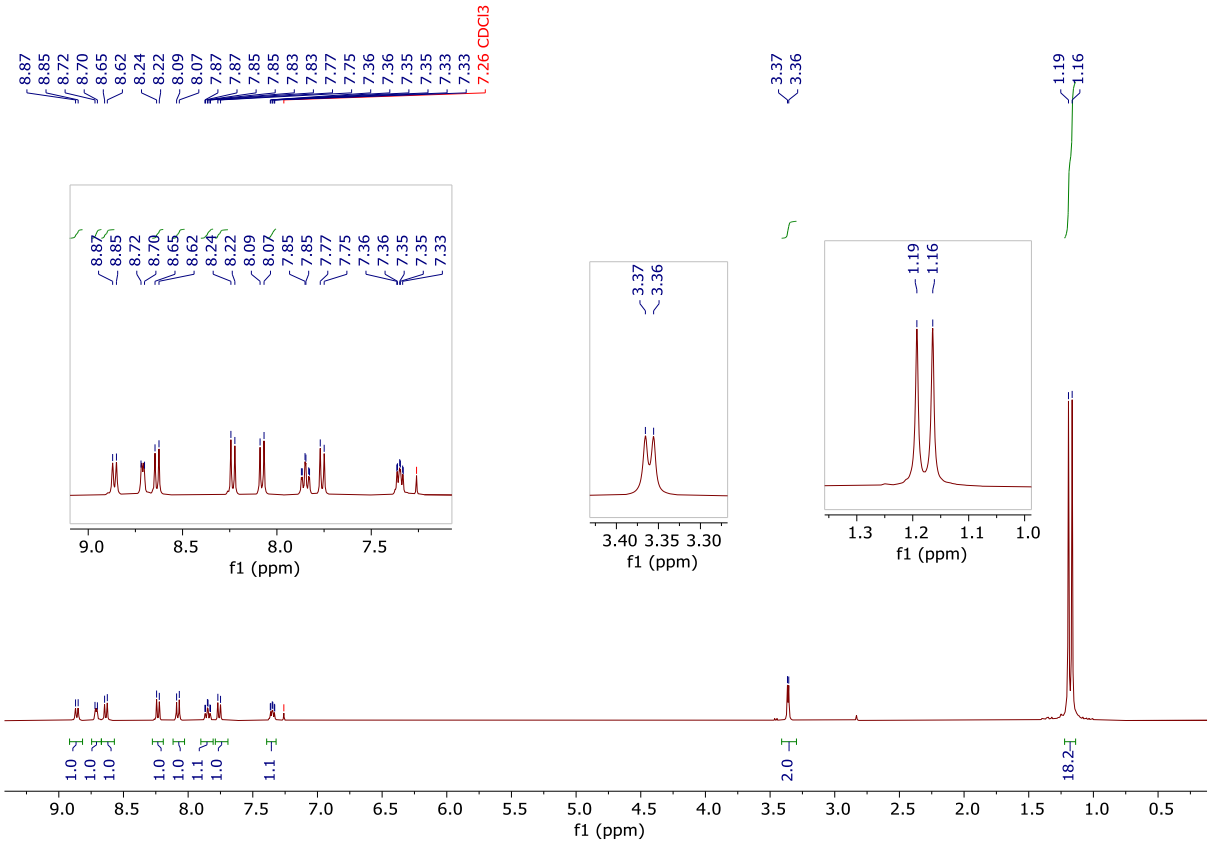

Figure S1. ^{1}H NMR spectrum of PNNN (400 MHz, $CDCl_3$, 298 K).

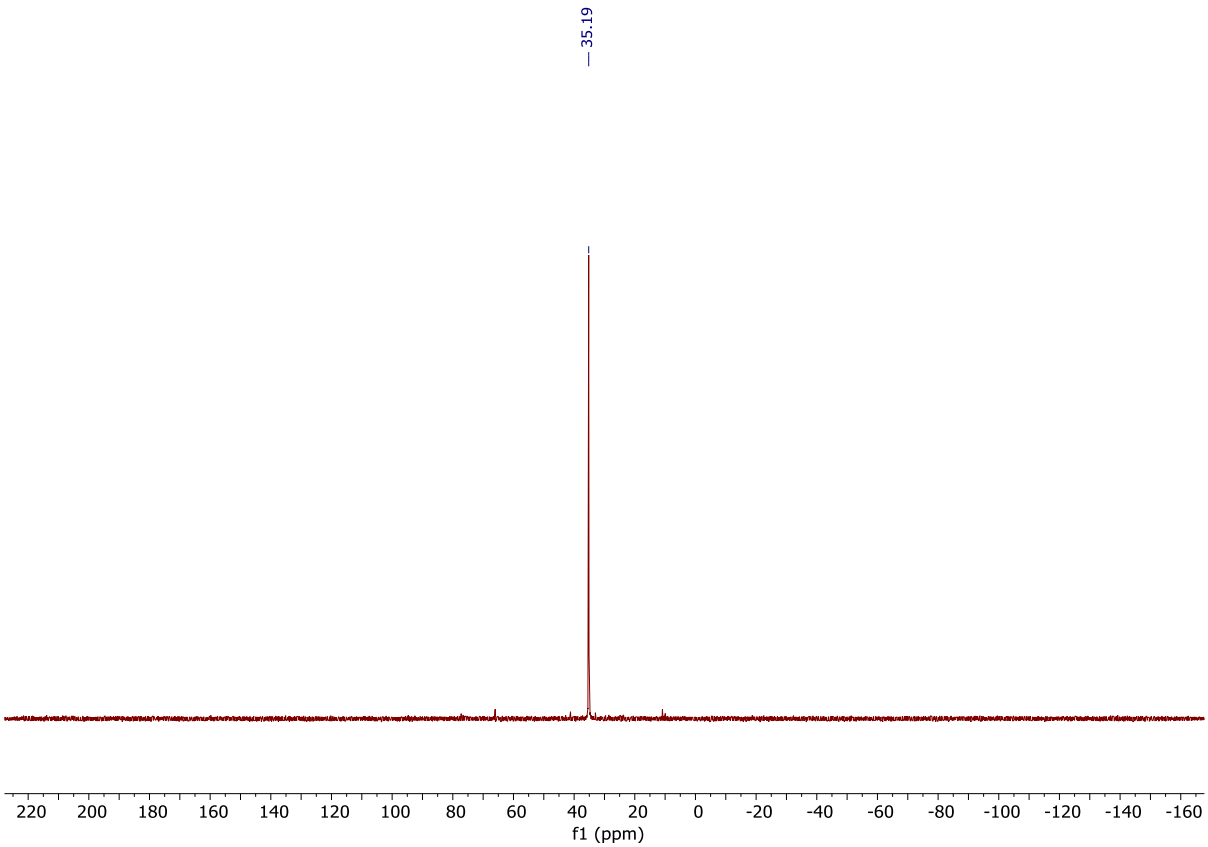

Figure S2. ^{31}P{^{1}H} NMR spectrum of PNNN (162 MHz, $CDCl_3$, 298 K).

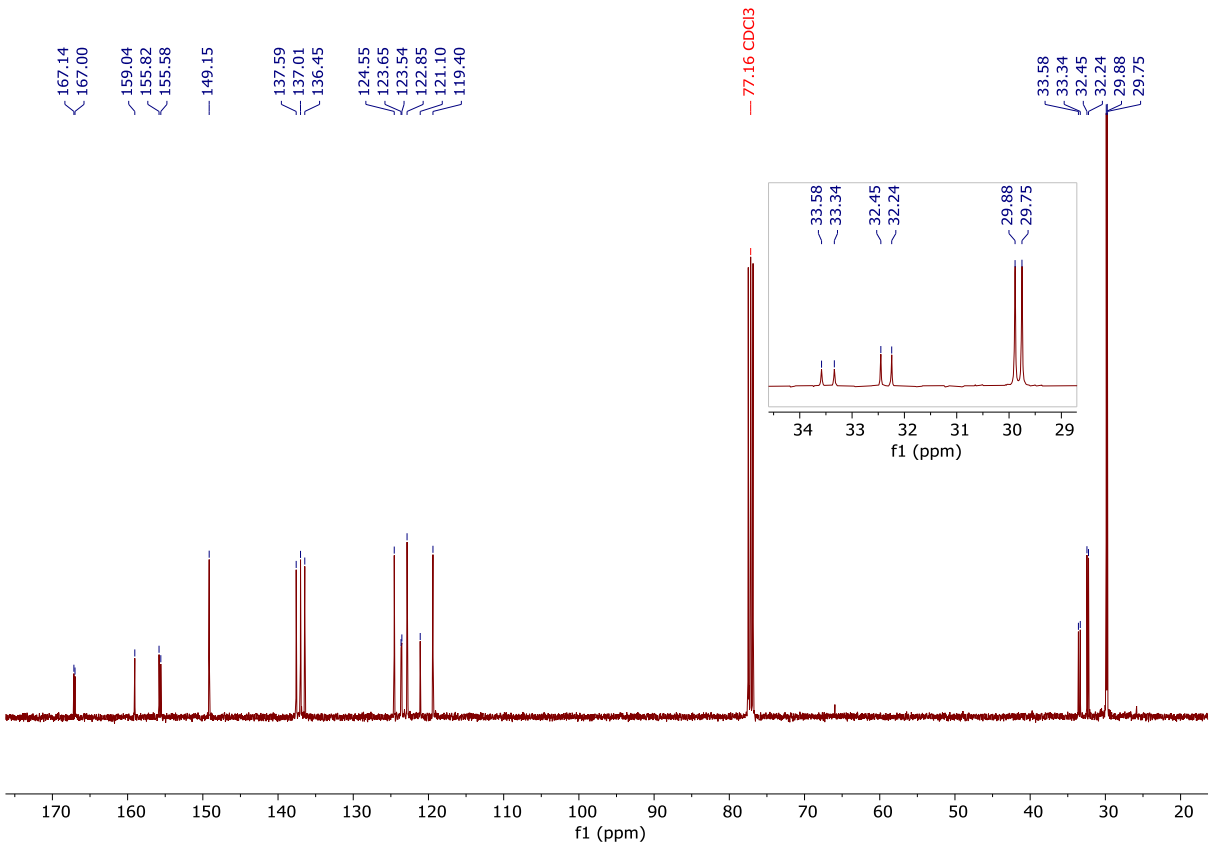

Figure S3. $^{13}C\{^{1}H\}$ NMR spectrum of PNNN (101 MHz, $CDCl_3$, 298 K).

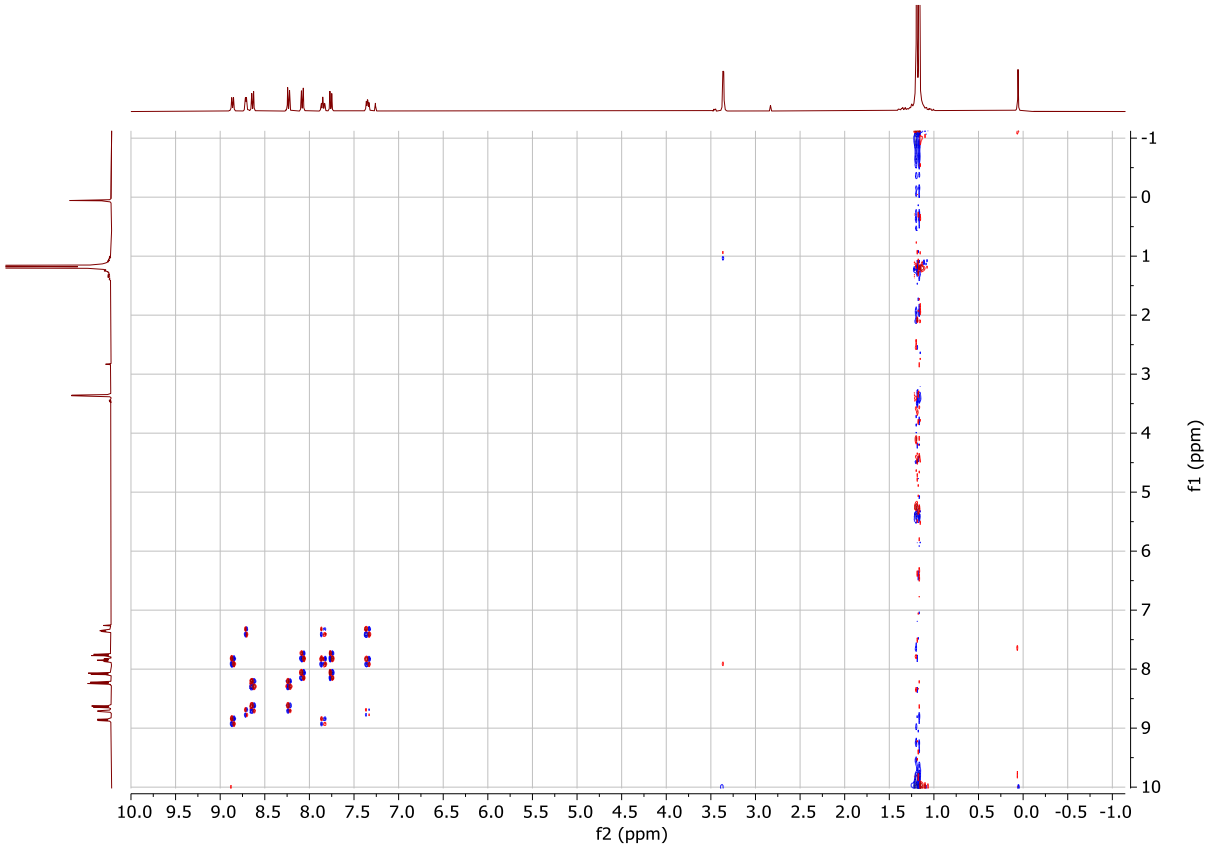

Figure S4. ^{1}H-^{1}H COSY NMR spectrum of PNNN (400 MHz, $CDCl_3$, 298 K).

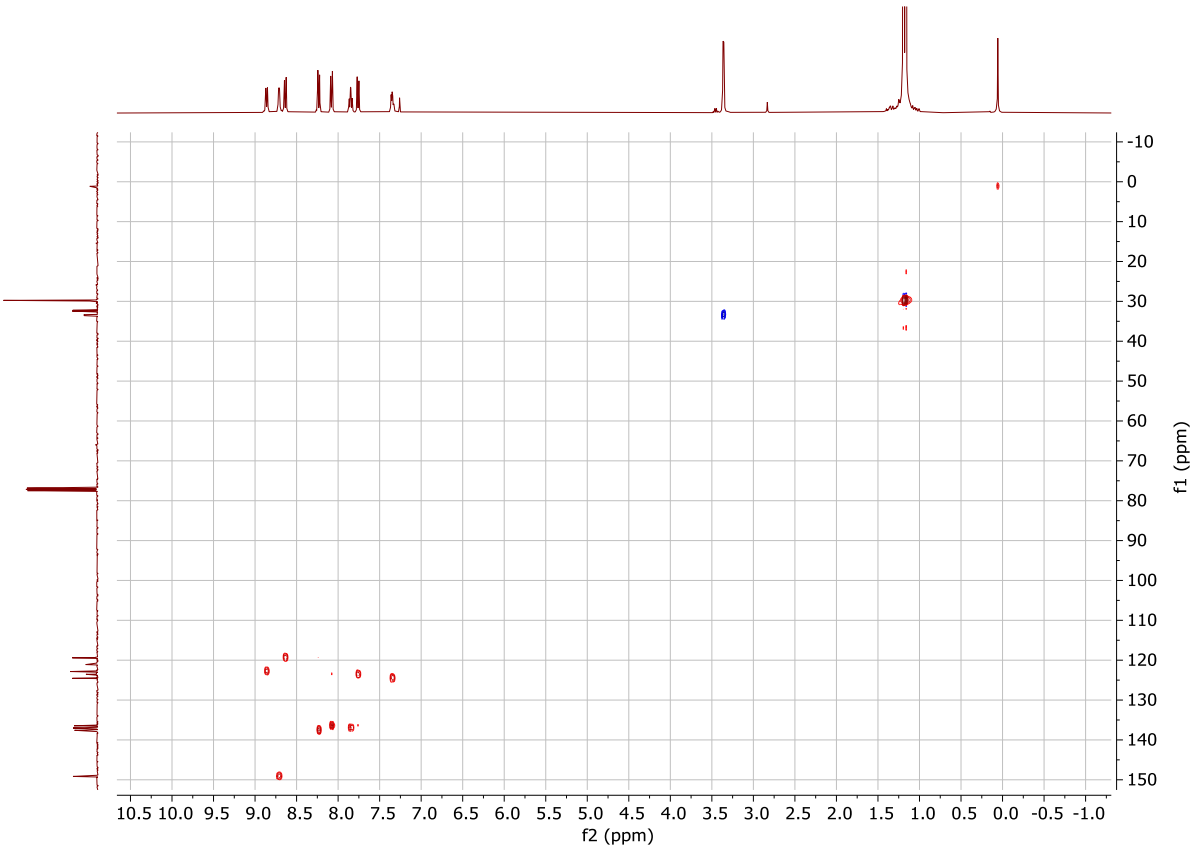

Figure S5. ^{1}H-^{13}C HSQC NMR spectrum of PNNN (101, 400 MHz, $CDCl_3$, 298 K).

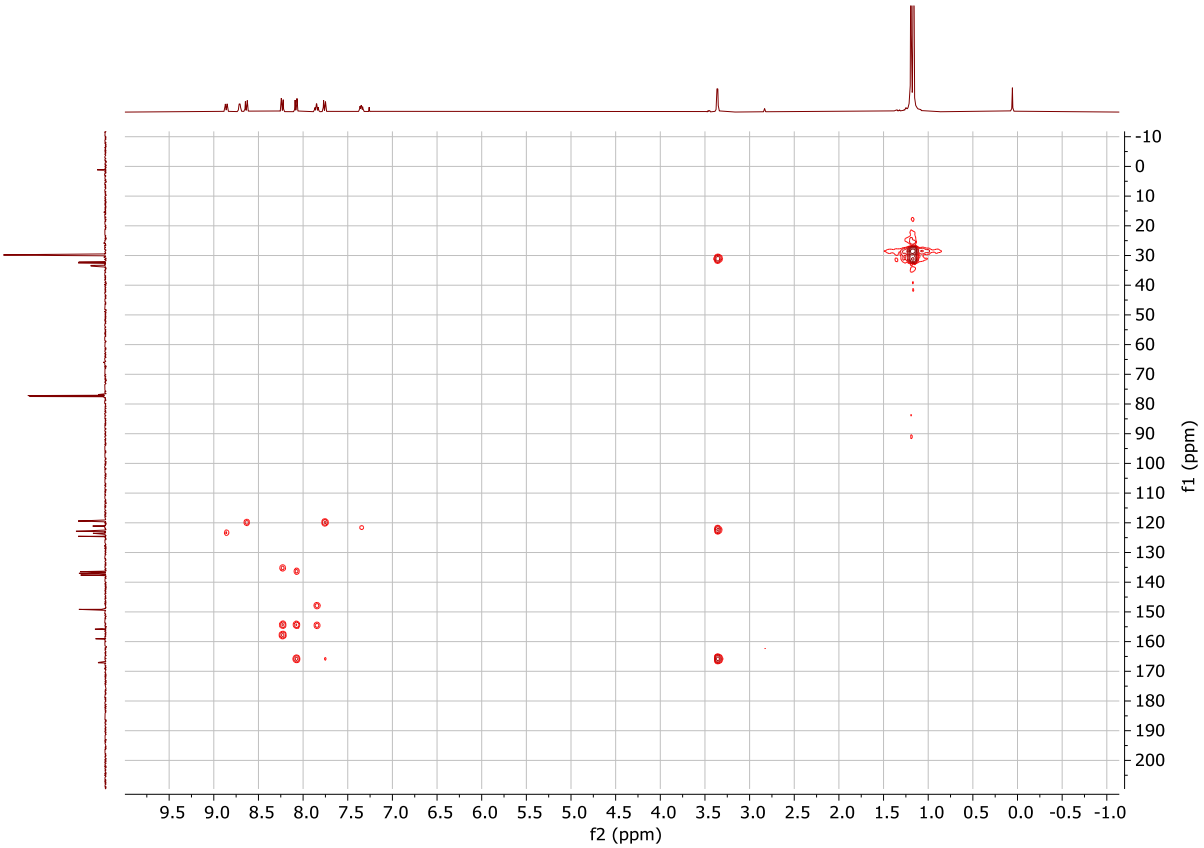

Figure S6. ^{1}H-^{13}C HMBC NMR spectrum of PNNN (101, 400 MHz, $CDCl_3$, 298 K).

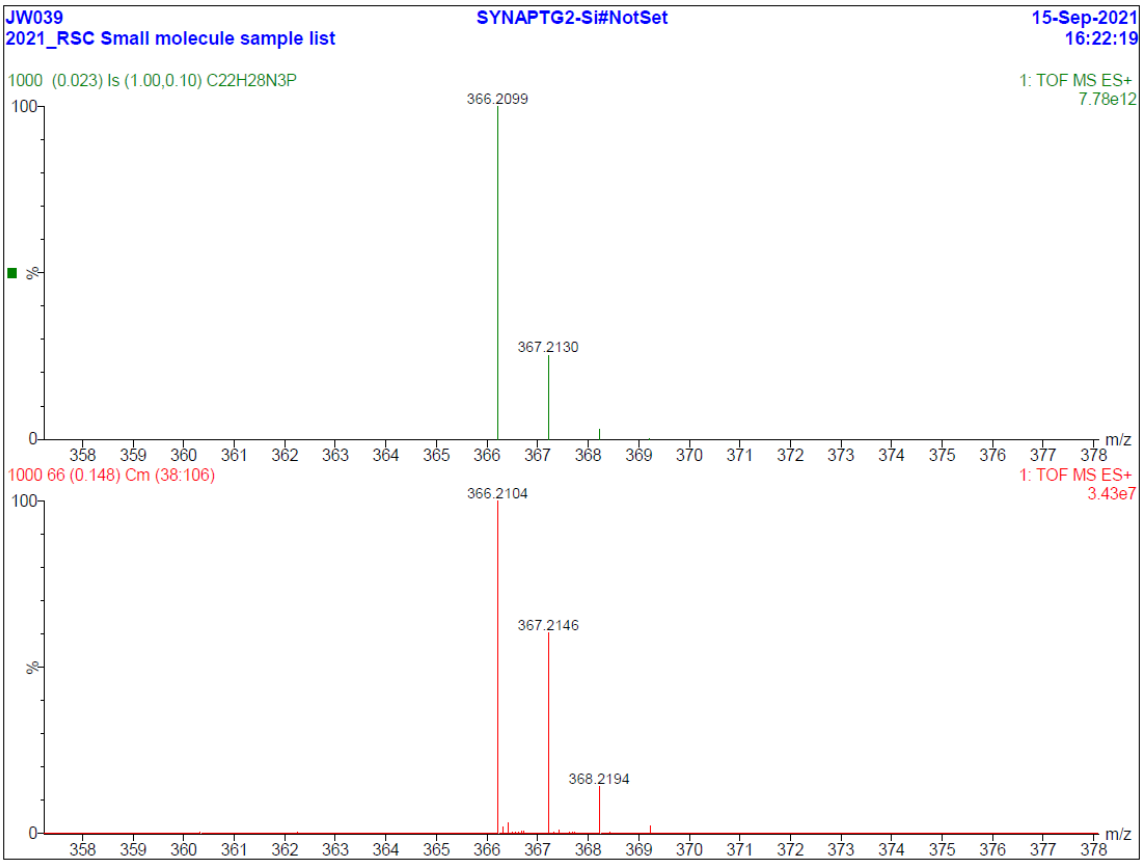

Figure S7. Experimental (bottom) and simulated (top) high resolution mass spectra (ESI+) of PNNN.

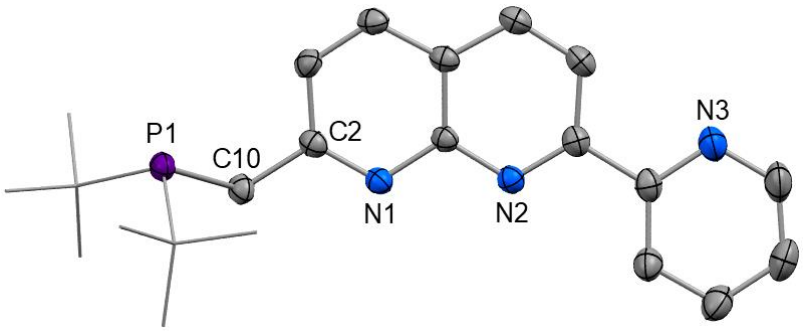

Figure S8. X-ray crystal structure of PNNN (50% displacement ellipsoids, H atoms and $CHCl_3$ solvent omitted). Selected bond lengths (Å) and degrees (°): P1–C10 1.869(2), C2–C10 1.506(3), N1–C2 1.322(3), P1–C10–C2 114.72(19).

2. Characterisation data for $[Cu_2Cl_2(PNNN)]$ (1)

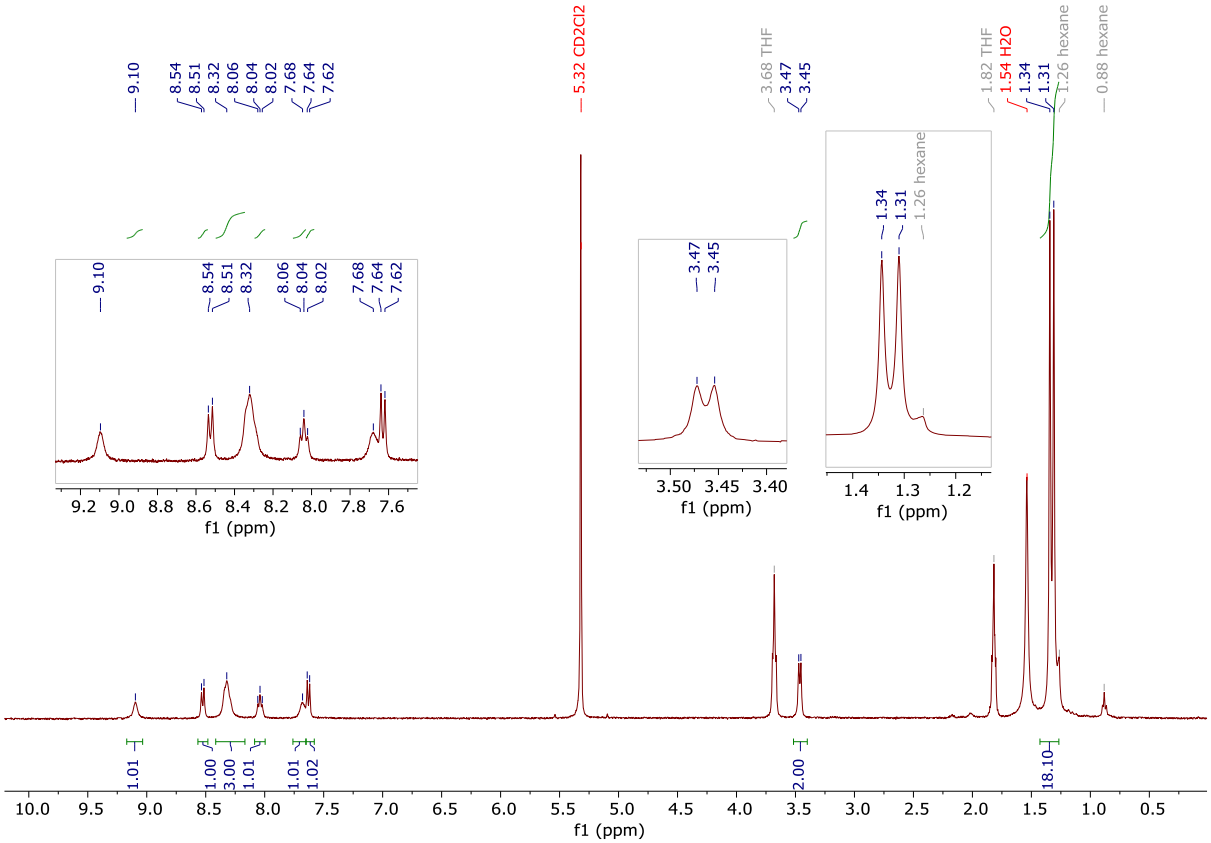

Figure S9. ^{1}H NMR spectrum of $[Cu_2Cl_2(PNNN)]$ (**1**) (400 MHz, CD_2Cl_2, 298 K).

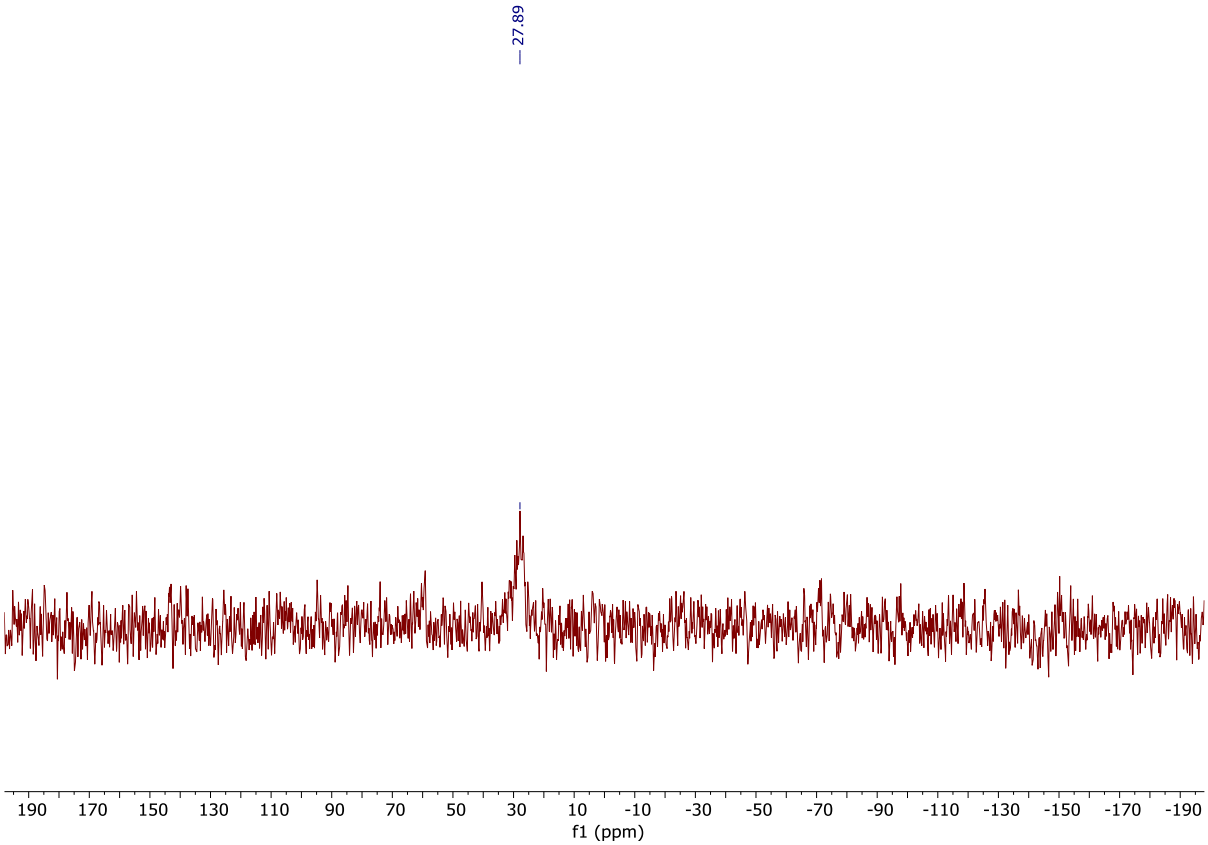

Figure S10. ^{31}P{^{1}H} NMR spectrum of $[Cu_2Cl_2(PNNN)]$ (**1**) (162 MHz, CD_2Cl_2, 298 K).

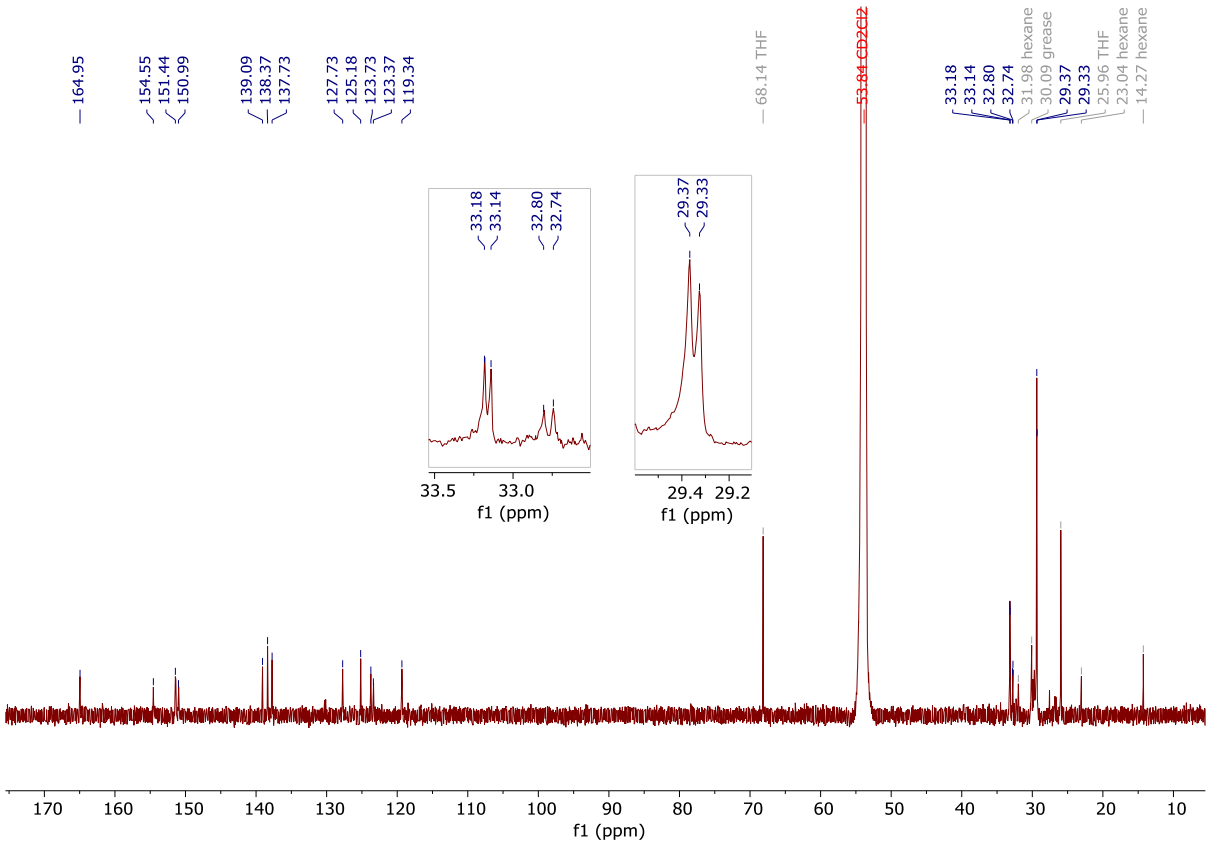

Figure S11. $^{13}C\{^{1}H\}$ NMR spectrum of $[Cu_2Cl_2(PNNN)]$ (**1**) (201 MHz, CD_2Cl_2, 298 K).

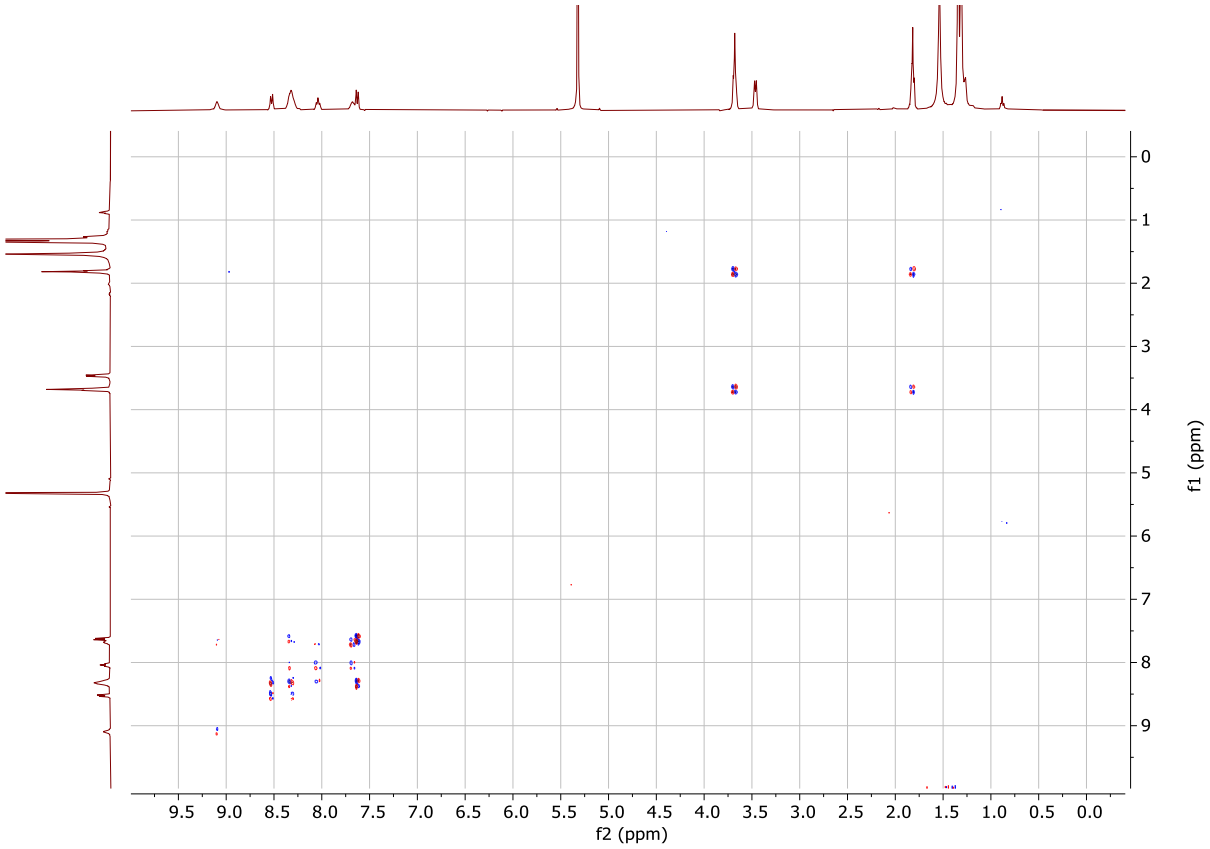

Figure S12. ^{1}H-^{1}H COSY NMR spectrum of $[Cu_2Cl_2(PNNN)]$ (**1**) (400 MHz, CD_2Cl_2, 298 K).

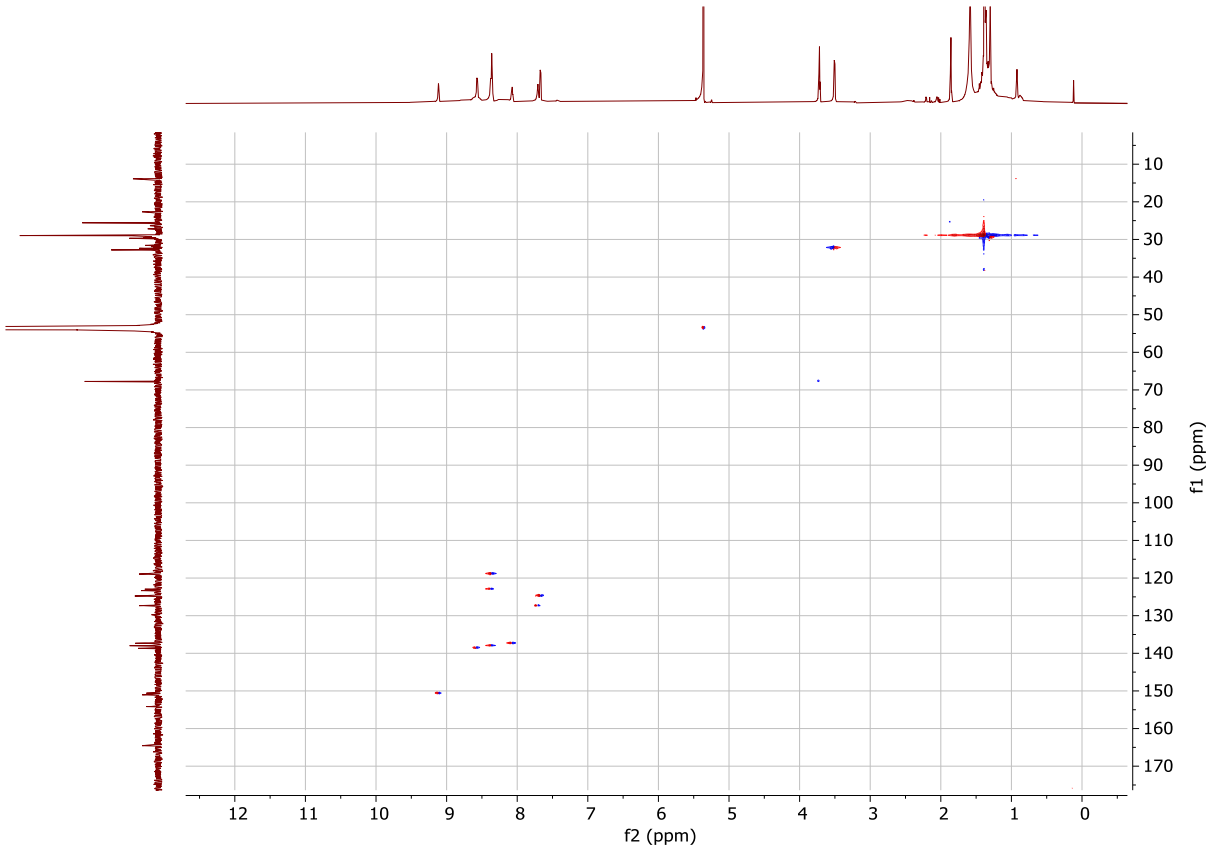

Figure S13. ^{1}H-^{13}C HSQC NMR spectrum of $[Cu_2Cl_2(PNNN)]$ (**1**) (201, 800 MHz, CD_2Cl_2, 298 K).

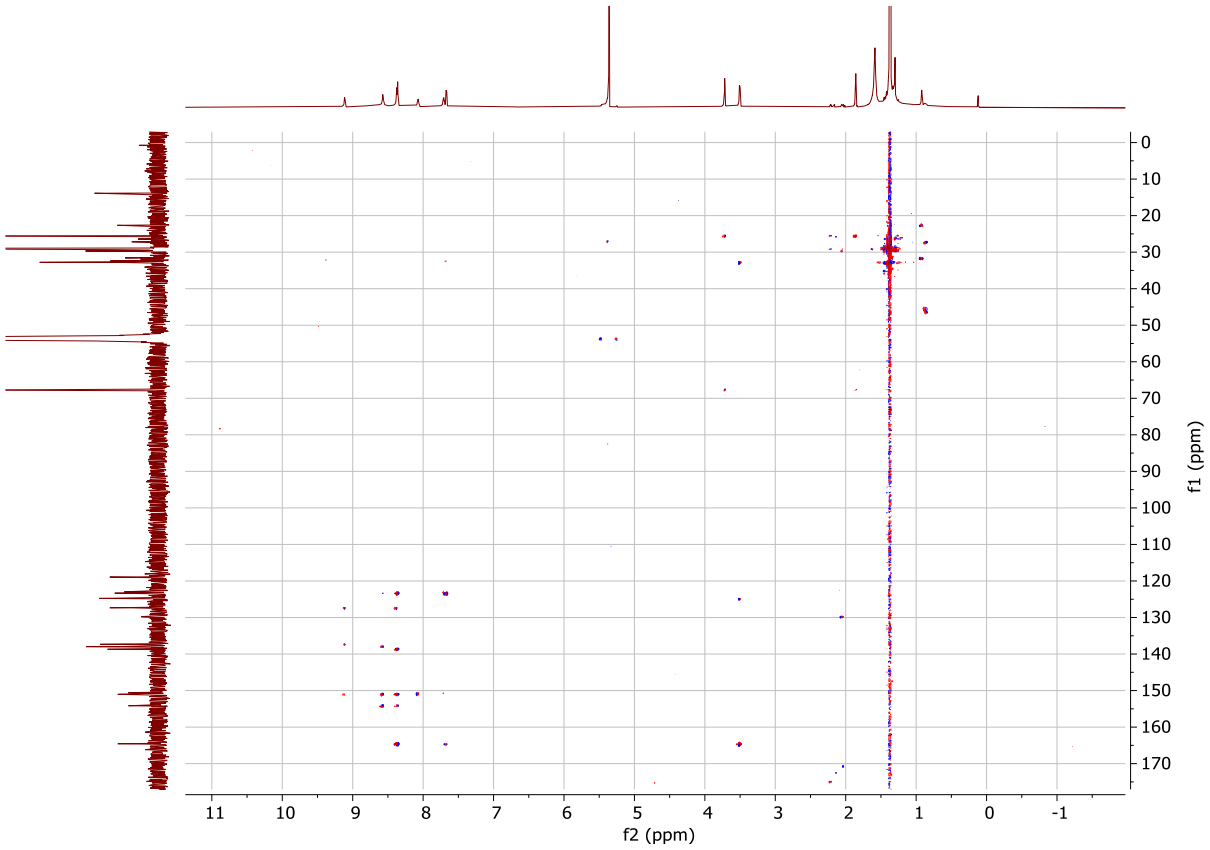

Figure S14. ^{1}H-^{13}C HMBC NMR spectrum of $[Cu_2Cl_2(PNNN)]$ (**1**) (201, 800 MHz, CD_2Cl_2, 298 K).

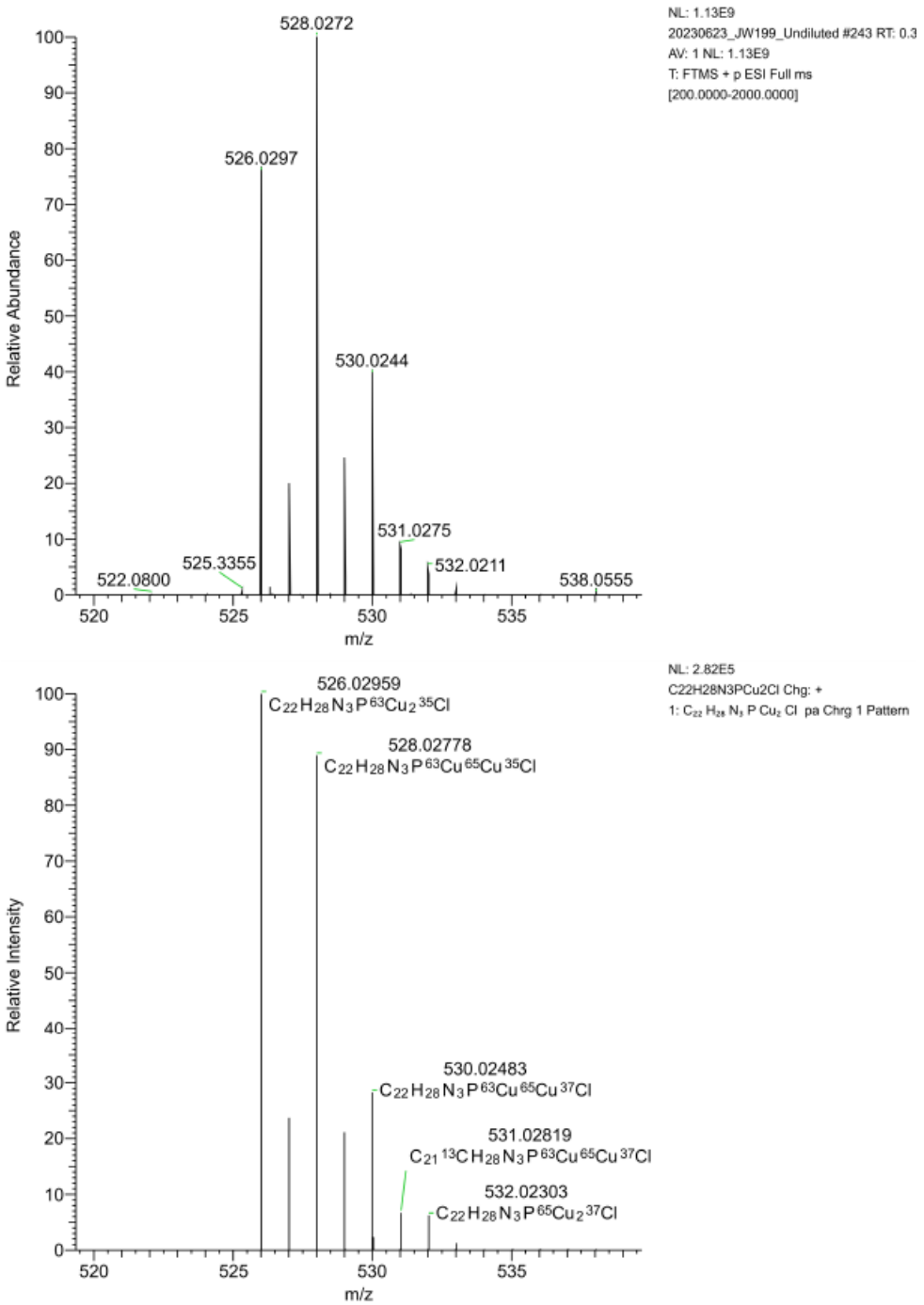

Figure S15. Experimental (top) and simulated (bottom) high resolution mass spectra (ESI+) of $[Cu_2Cl_2(PNNN)]$ (**1**).

3. Characterisation data for [RuCl(cymene)(PNNN)]Cl ([2]Cl)

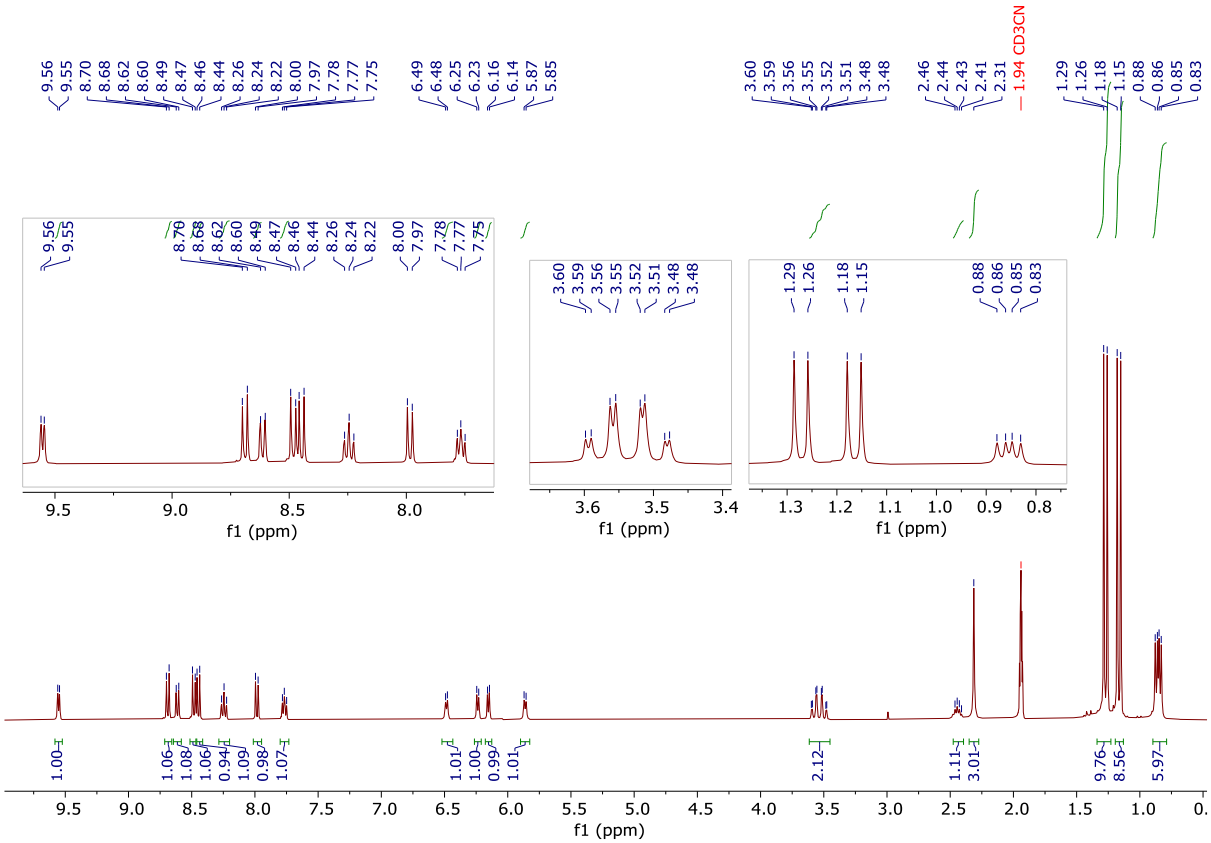

Figure S16. ^{1}H NMR spectrum of [RuCl(cymene)(PNNN)]Cl (**[2]Cl**) (400 MHz, CD_3CN, 298 K).

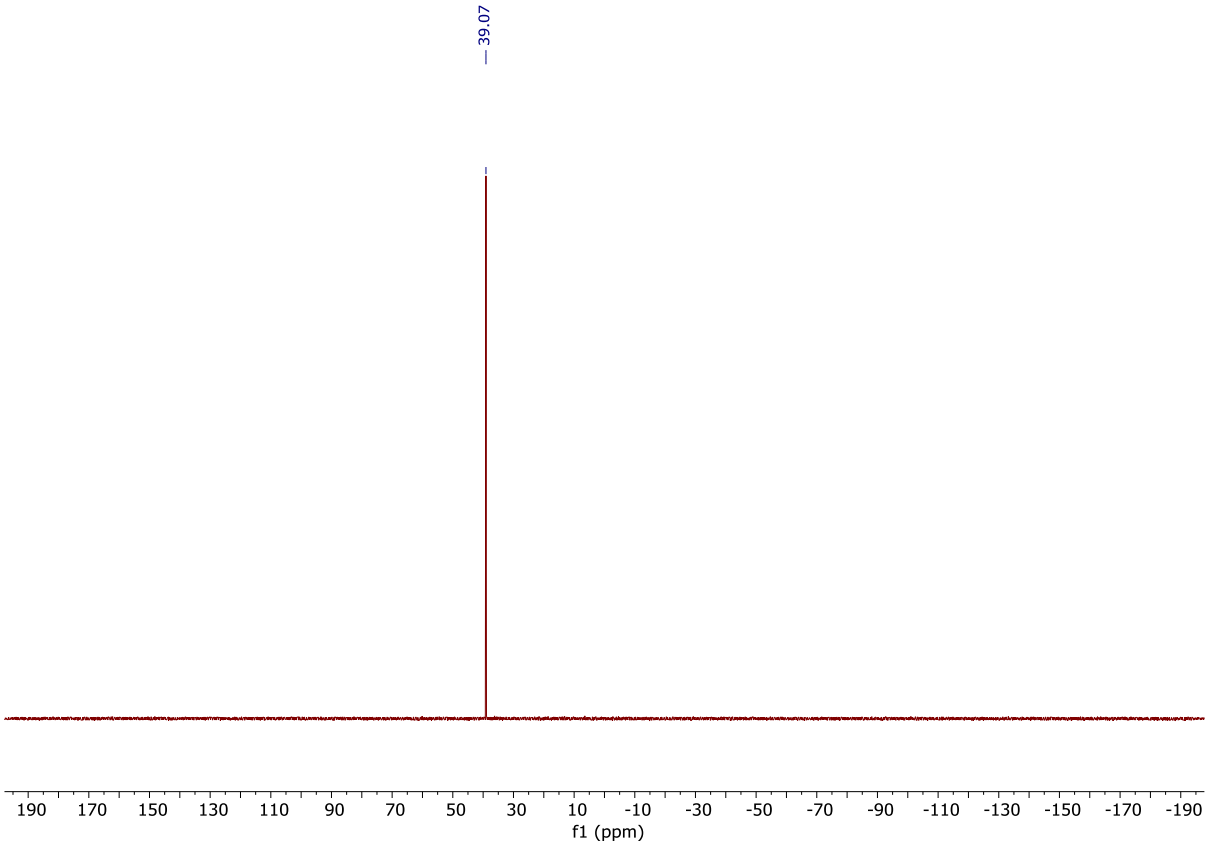

Figure S17. ^{31}P{^{1}H} NMR spectrum of [RuCl(cymene)(PNNN)]Cl (**[2]Cl**) (162 MHz, CD_3CN, 298 K).

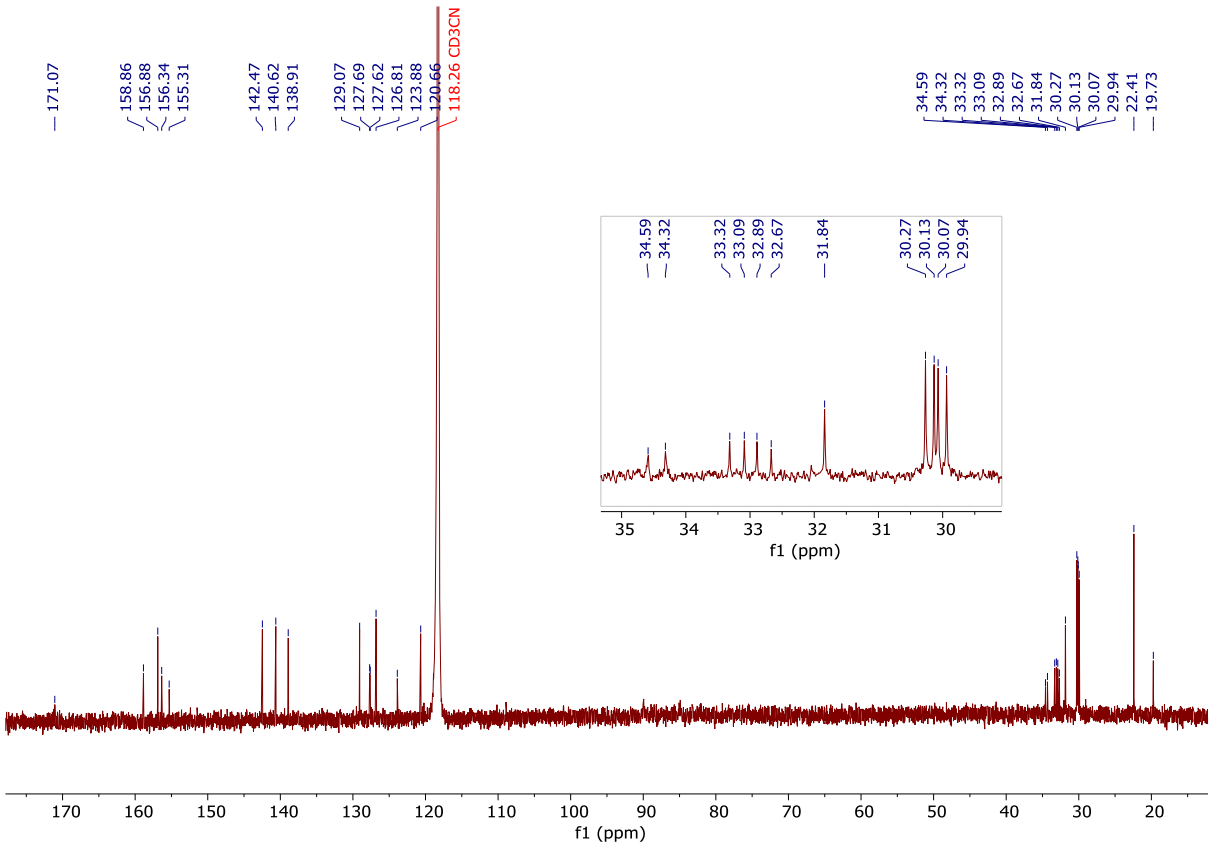

Figure S18. $^{13}C\{^{1}H\}$ NMR spectrum of [RuCl(cymene)(PNNN)]Cl (**[2]Cl**) (101 MHz, CD_3CN, 298 K).

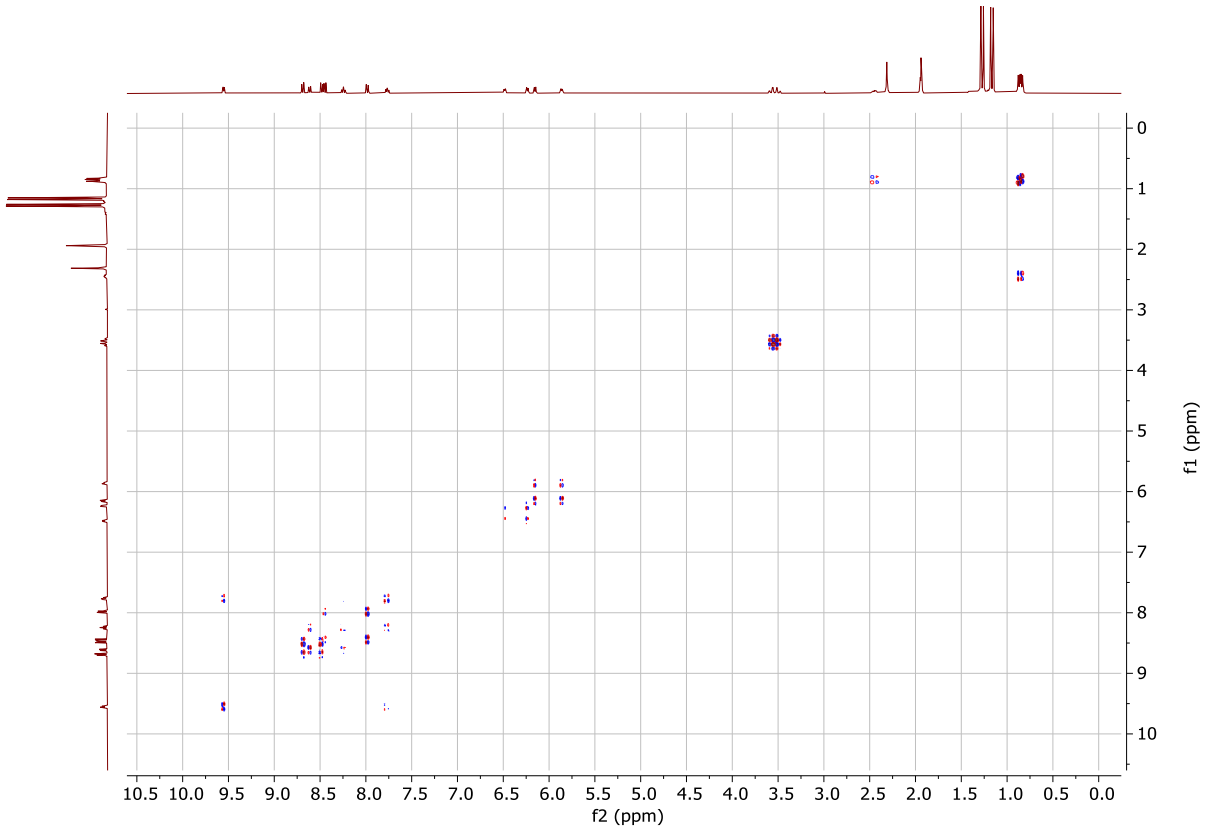

Figure S19. ^{1}H-^{1}H COSY NMR spectrum of [RuCl(cymene)(PNNN)]Cl (**[2]Cl**) (400 MHz, CD_3CN, 298 K).

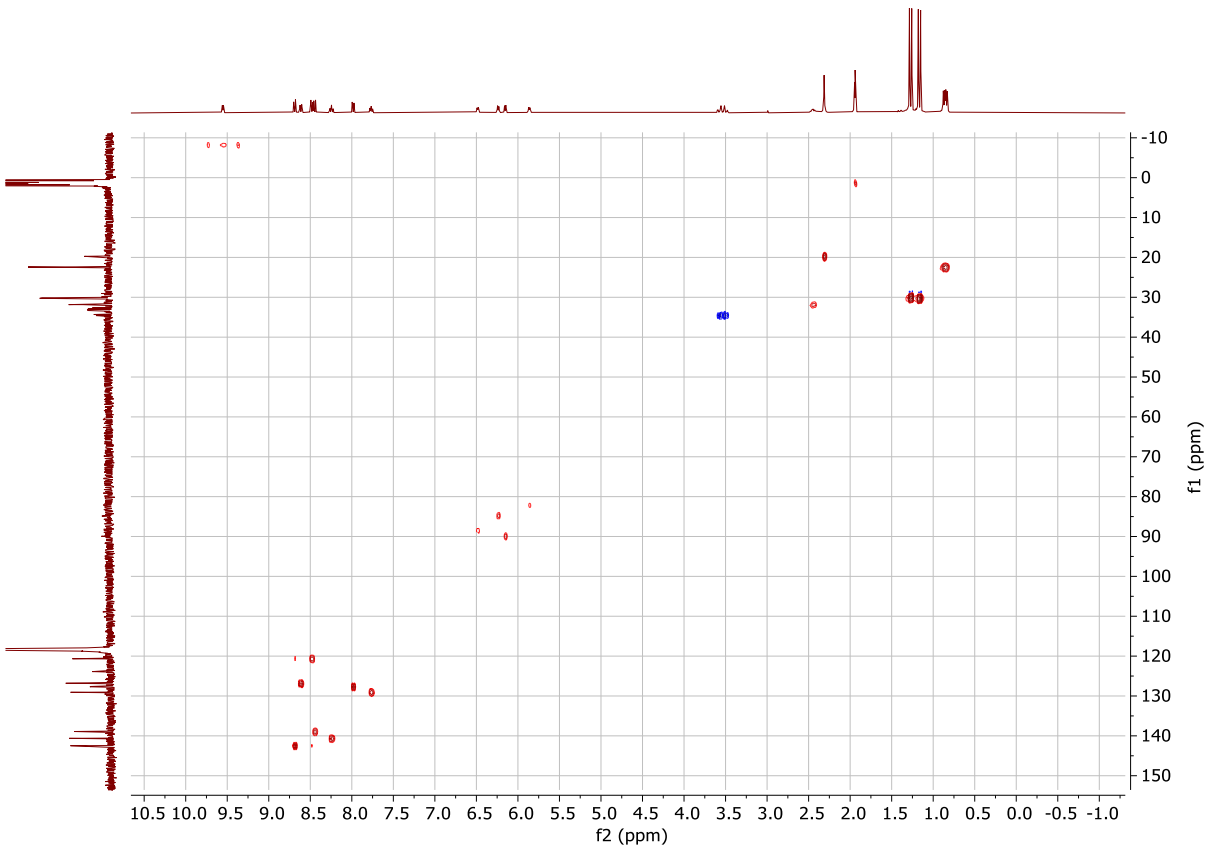

Figure S20. ^{1}H-^{13}C HSQC NMR spectrum of [RuCl(cymene)(PNNN)]Cl (**[2]Cl**) (101, 400 MHz, CD_3CN, 298 K).

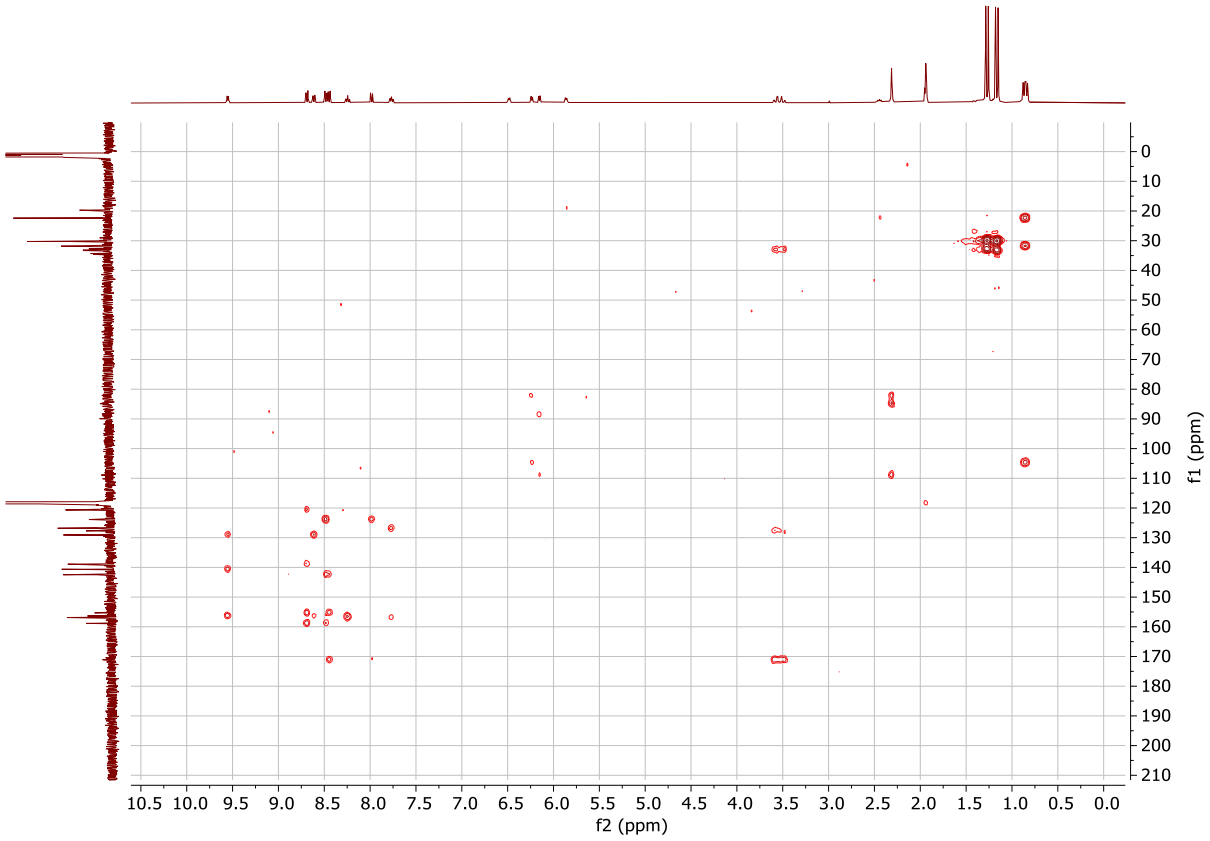

Figure S21. ^{1}H-^{13}C HMBC NMR spectrum of [RuCl(cymene)(PNNN)]Cl (**[2]Cl**) (101, 400 MHz, CD_3CN, 298 K).

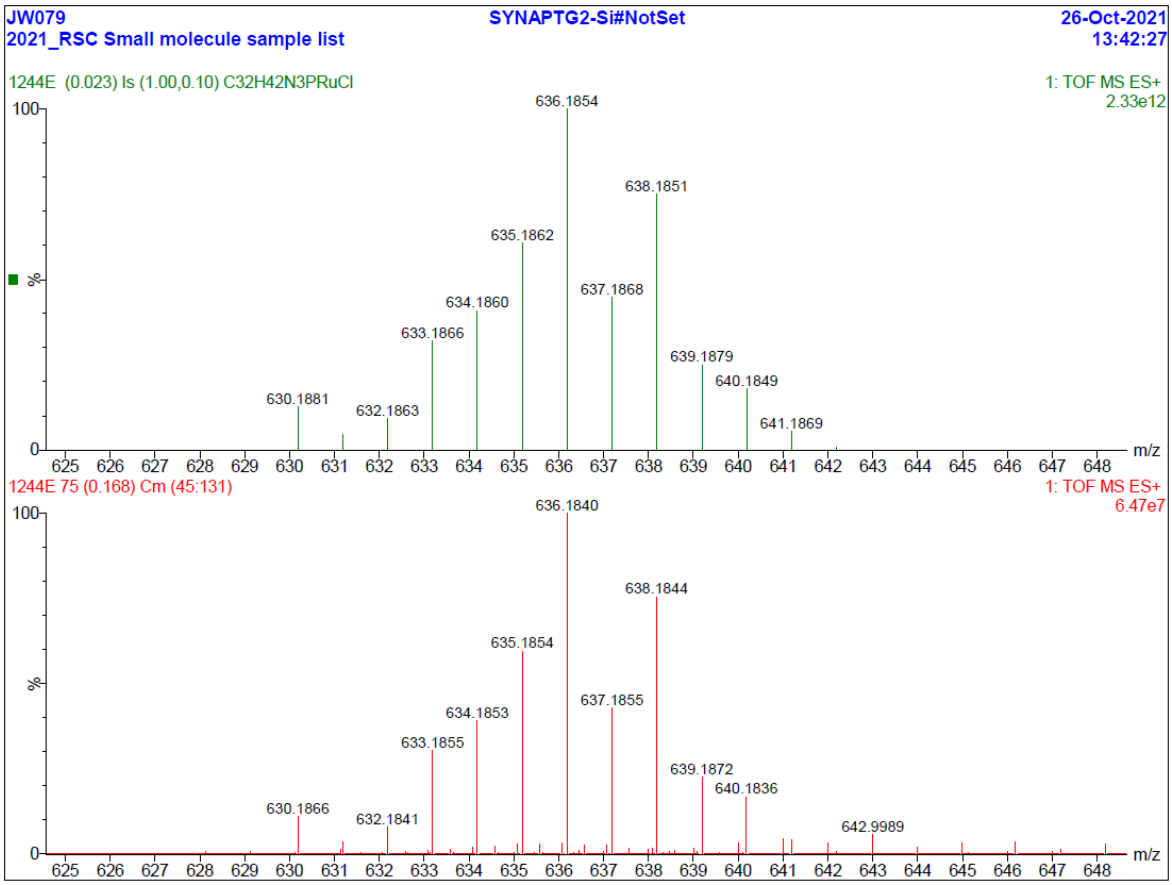

Figure S22. Experimental (bottom) and simulated (top) high resolution mass spectra (ESI+) of [RuCl(cymene)(PNNN)]Cl (**[2]Cl**).

4. Characterisation data for [RuCl(cymene)(PNNN)]PF_6 ([2]PF_6)

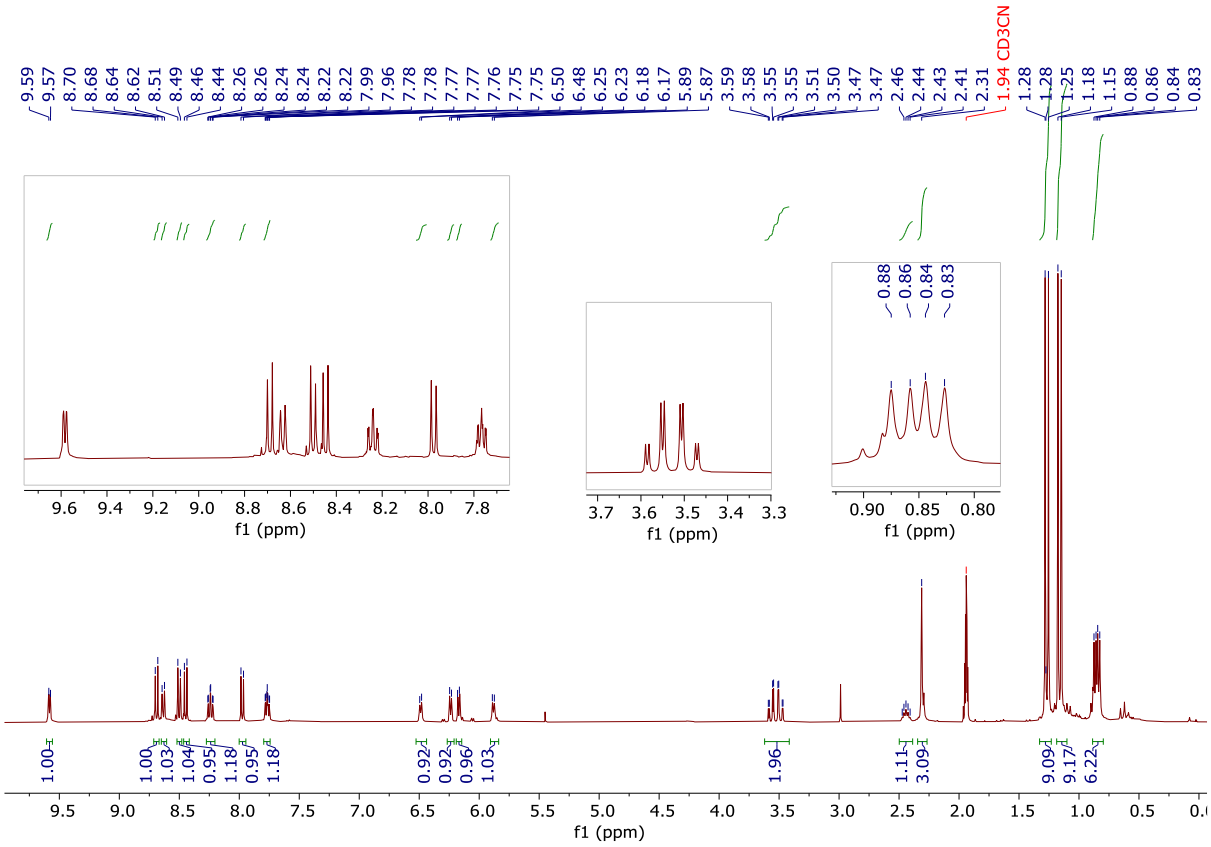

Figure S23. ^{1}H NMR spectrum of [RuCl(cymene)(PNNN)]PF_6 (**[2]PF_6**) (400 MHz, CD_3CN, 298 K).

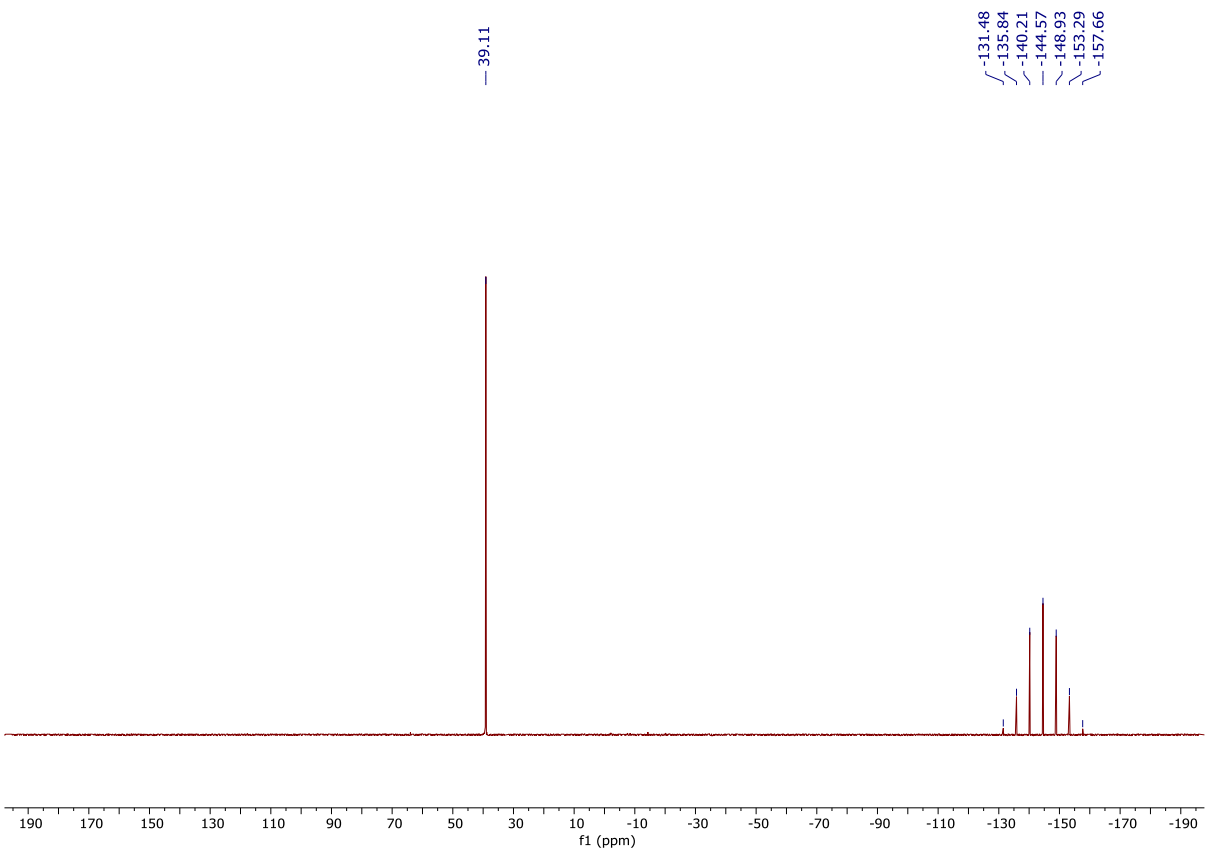

Figure S24. ^{31}P{^{1}H} NMR spectrum of [RuCl(cymene)(PNNN)]PF_6 (**[2]PF_6**) (162 MHz, CD_3CN, 298 K).

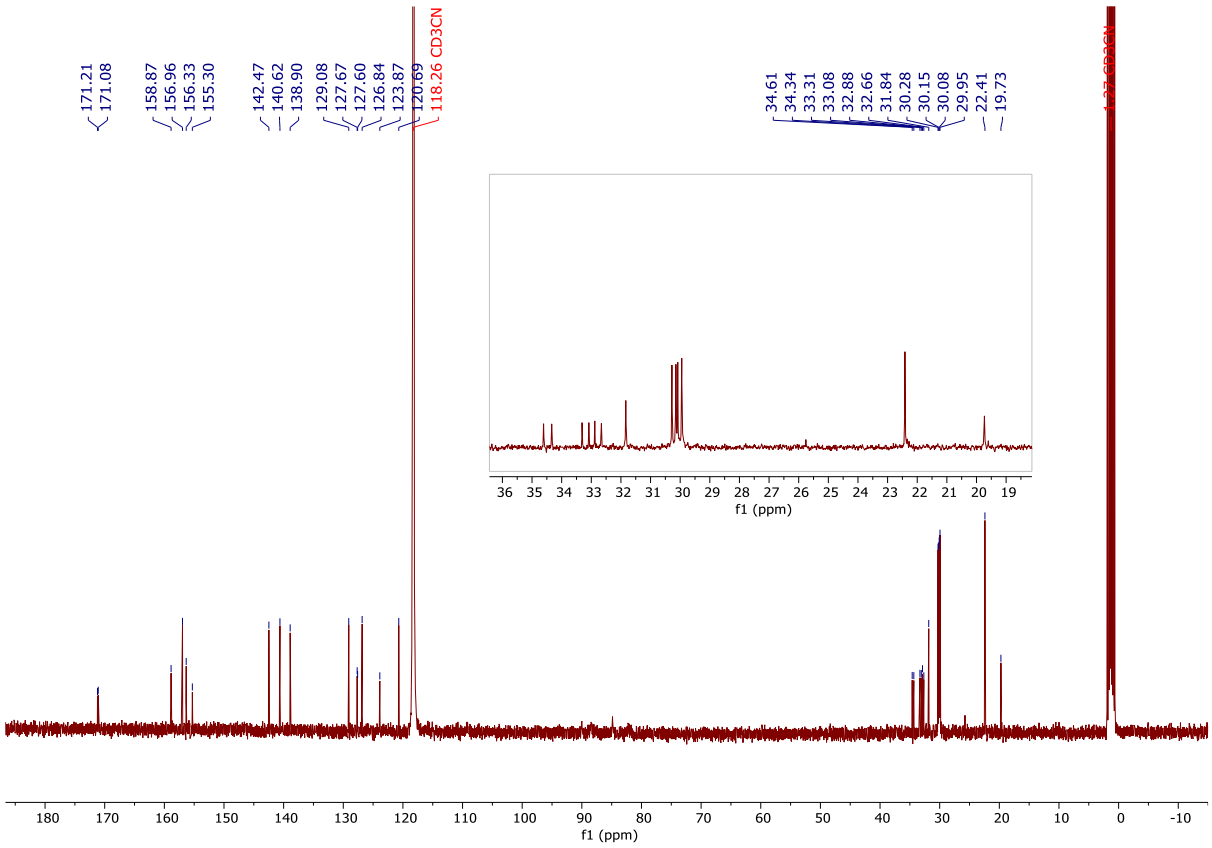

Figure S25. $^{13}C\{^{1}H\}$ NMR spectrum of [RuCl(cymene)(PNNN)]PF_6 (**[2]PF$_6$**) (101 MHz, CD_3CN, 298 K).

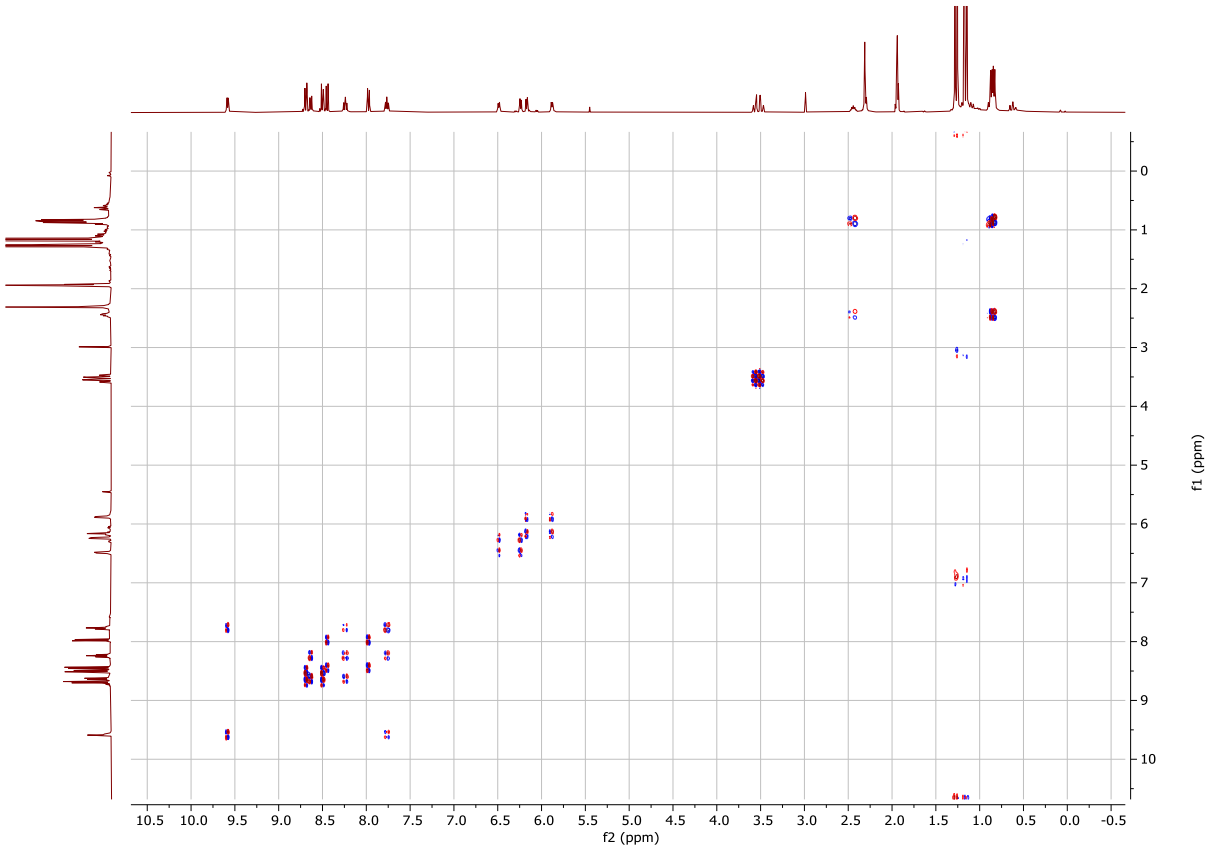

Figure S26. ^{1}H-^{1}H COSY NMR spectrum of [RuCl(cymene)(PNNN)]PF_6 (**[2]PF$_6$**) (400 MHz, CD_3CN, 298 K).

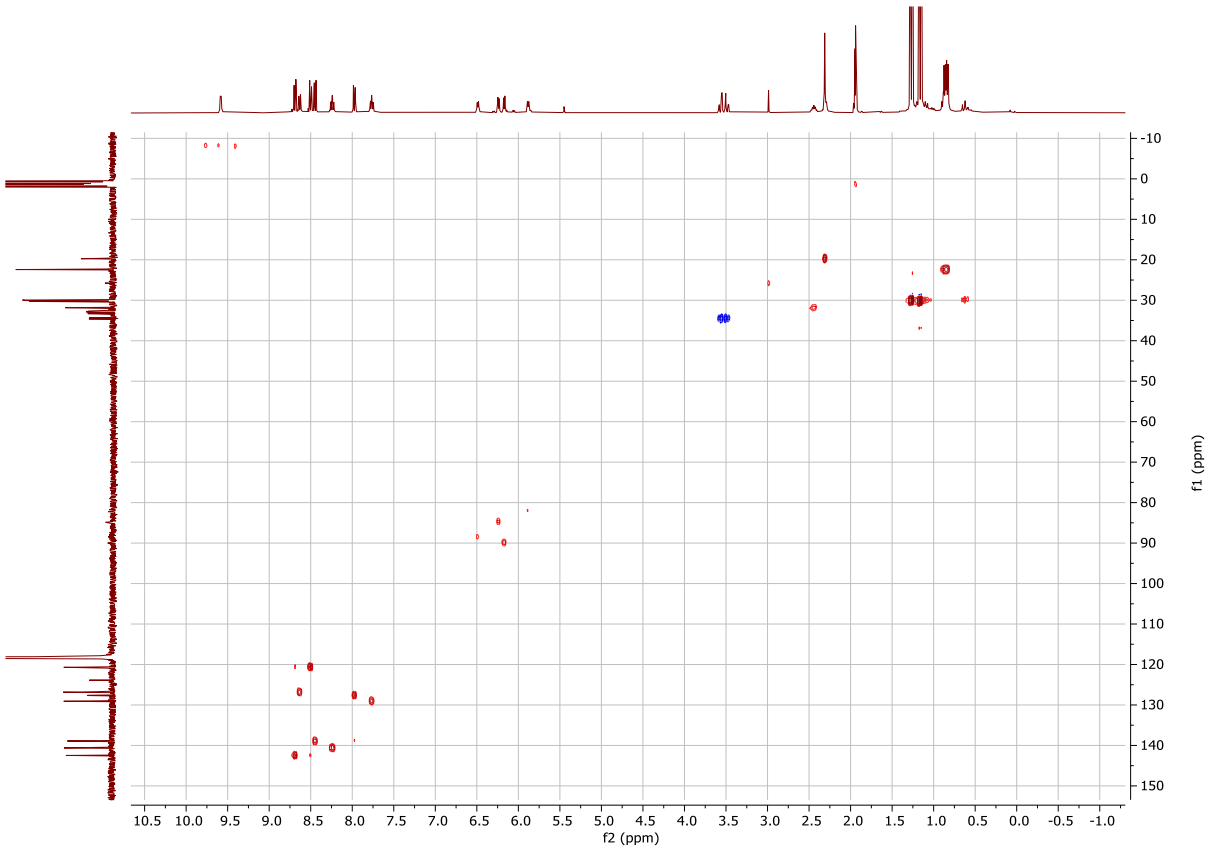

Figure S27. ^{1}H-^{13}C HSQC NMR spectrum of [RuCl(cymene)(PNNN)]PF_6 (**[2]PF_6**) (101, 400 MHz, CD_3CN, 298 K).

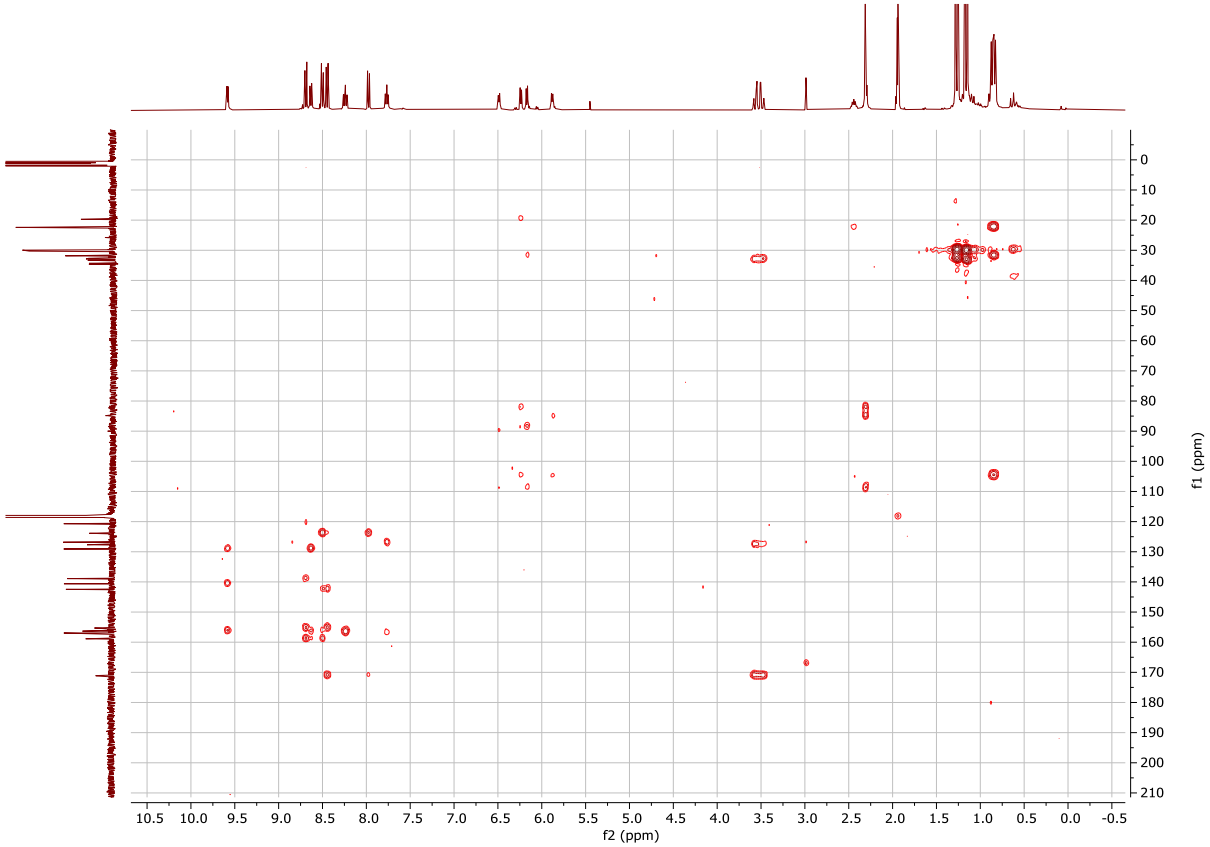

Figure S28. ^{1}H-^{13}C HMBC NMR spectrum of [RuCl(cymene)(PNNN)]PF_6 (**[2]PF_6**) (101, 400 MHz, CD_3CN, 298 K).

5. Characterisation data for [RuCuCl$_3$(cymene)(PNNN)] (3)

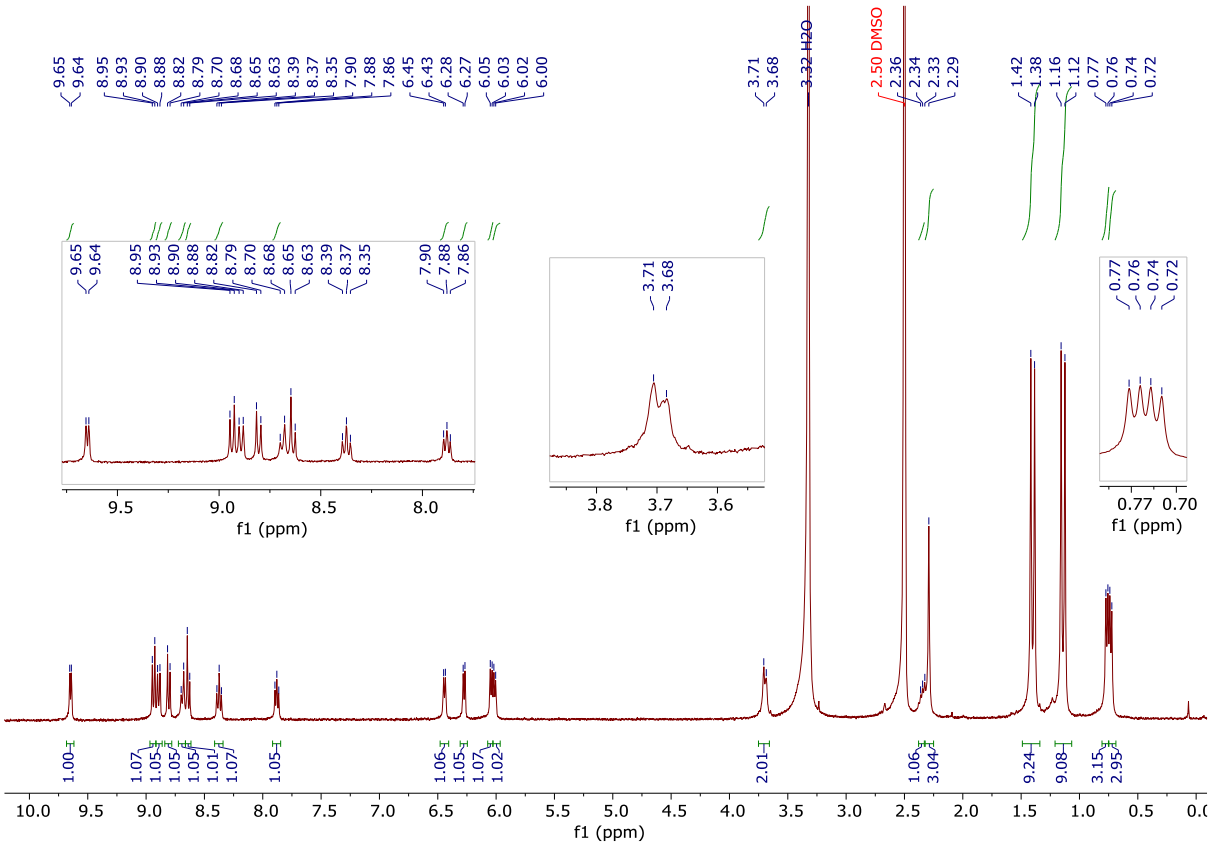

Figure S29. ^{1}H NMR spectrum of [RuCuCl$_3$(cymene)(PNNN)] (**3**) (400 MHz, $(CD_3)_2SO$, 298 K).

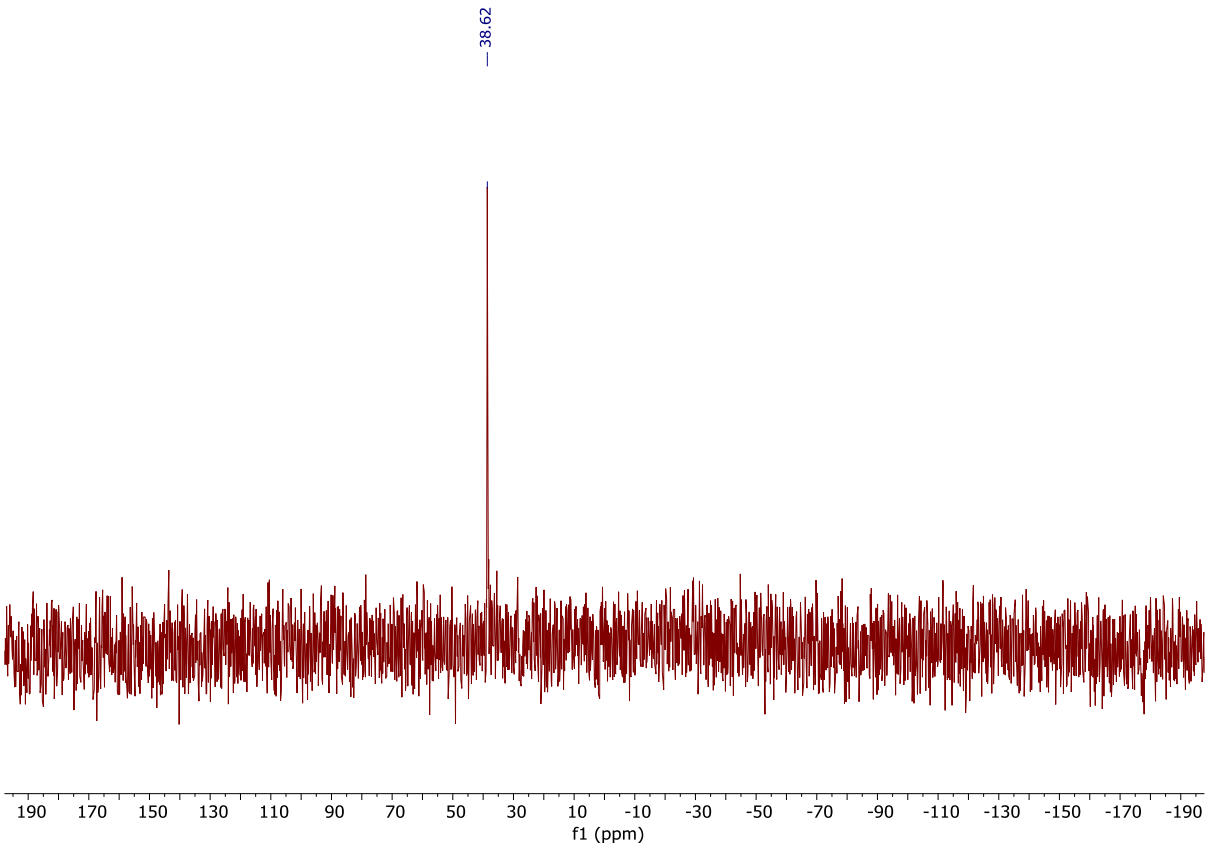

Figure S30. ^{31}P{^{1}H} NMR spectrum of [RuCuCl$_3$(cymene)(PNNN)] (**3**) (162 MHz, $(CD_3)_2SO$, 298 K).

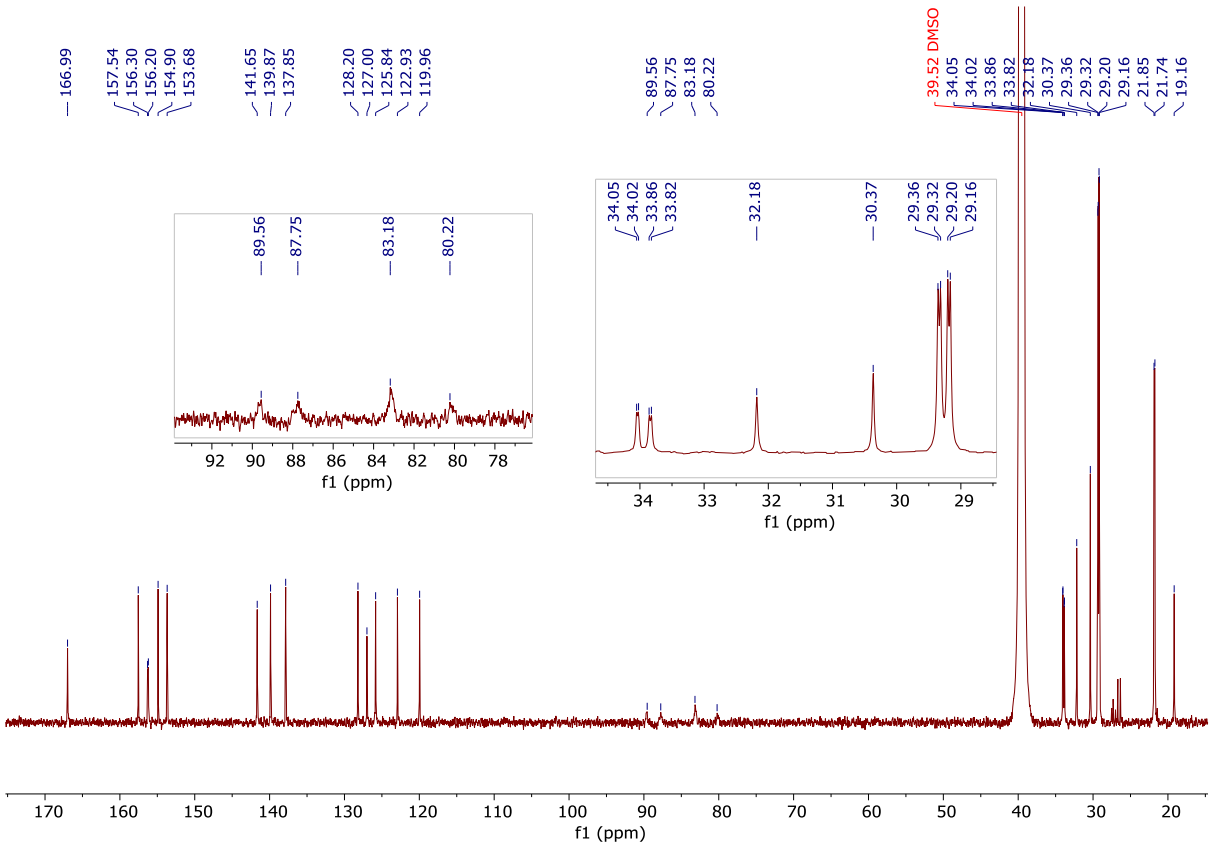

Figure S31. $^{13}C\{^{1}H\}$ NMR spectrum of [$RuCuCl_3$(cymene)(PNNN)] (**3**) (201 MHz, $(CD_3)_2SO$, 298 K).

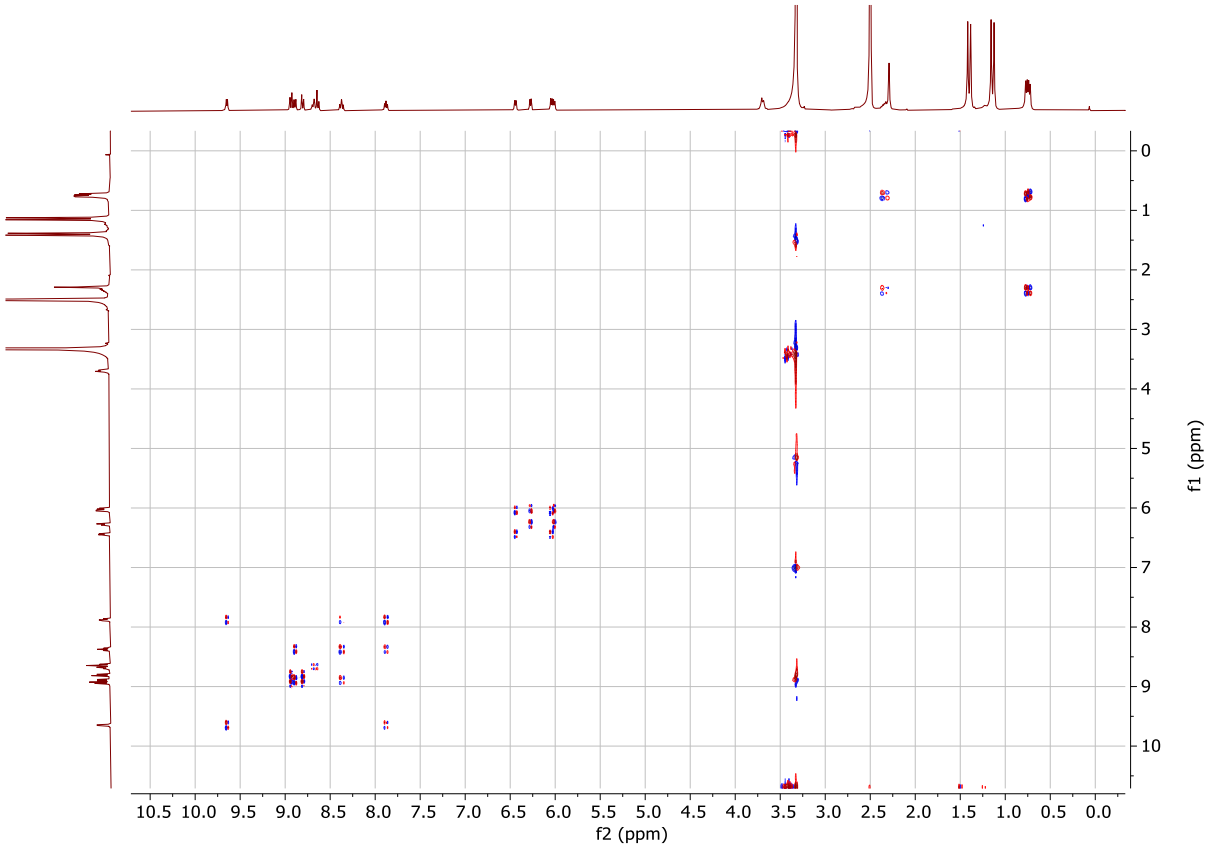

Figure S32. ^{1}H-^{1}H COSY NMR spectrum of [$RuCuCl_3$(cymene)(PNNN)] (**3**) (400 MHz, $(CD_3)_2SO$, 298 K).

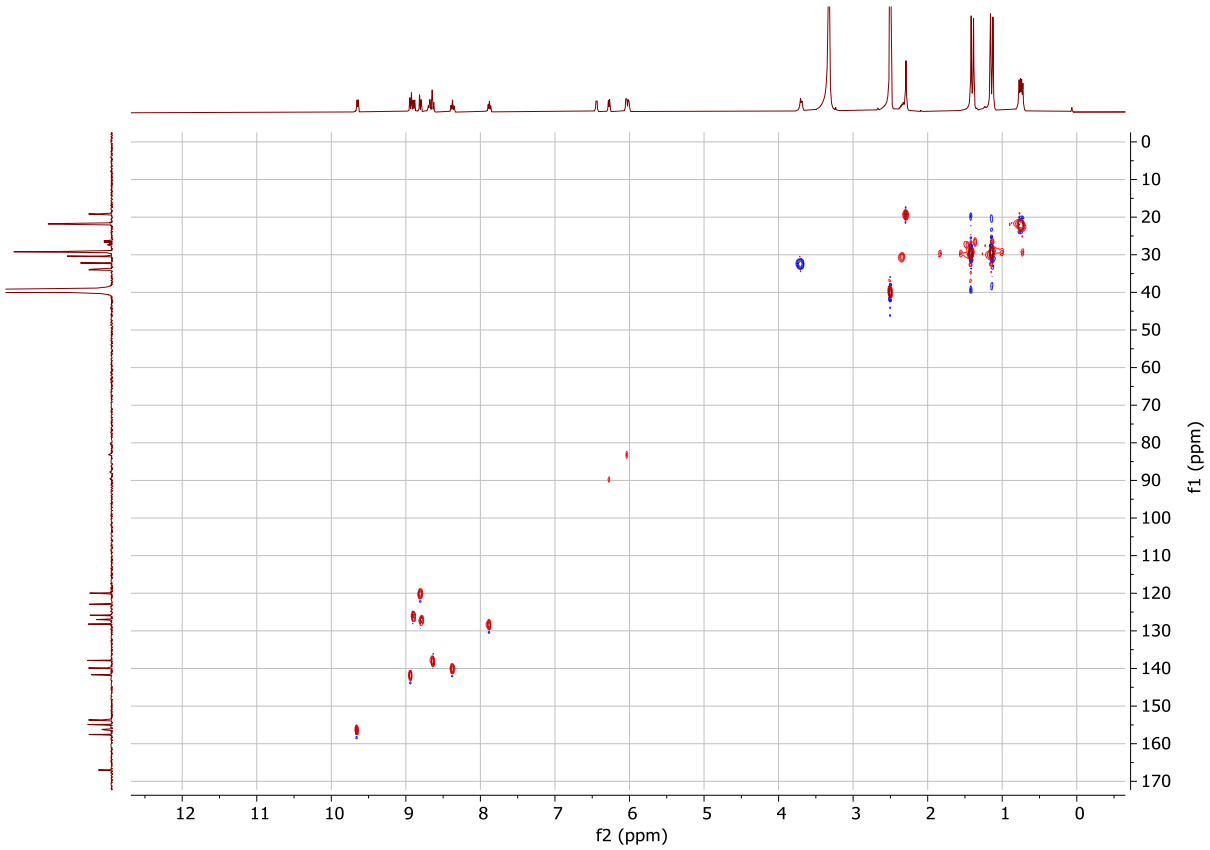

Figure S33. ^{1}H-^{13}C HSQC NMR spectrum of [$RuCuCl_3$(cymene)(PNNN)] (**3**) (201, 800 MHz, $(CD_3)_2SO$, 298 K).

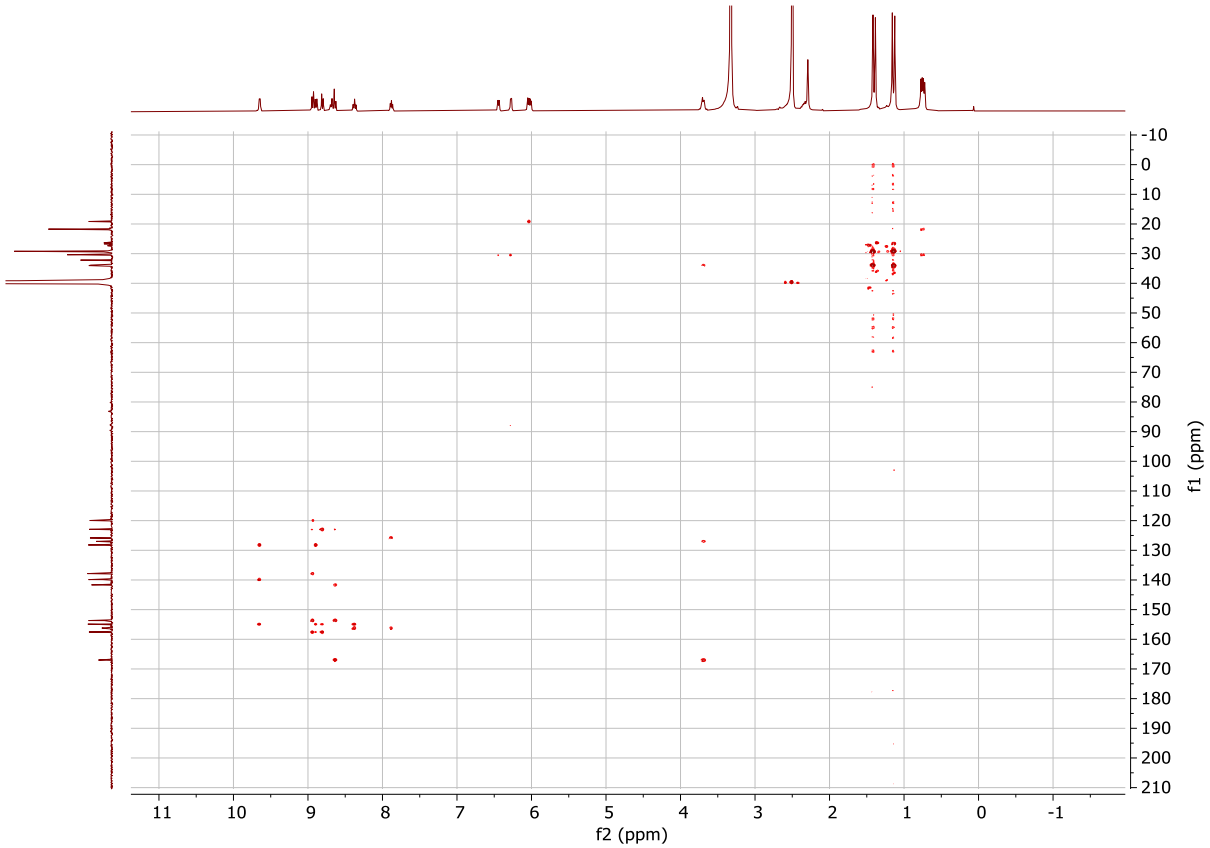

Figure S34. ^{1}H-^{13}C HMBC NMR spectrum of [$RuCuCl_3$(cymene)(PNNN)] (**3**) (201, 800 MHz, $(CD_3)_2SO$, 298 K).

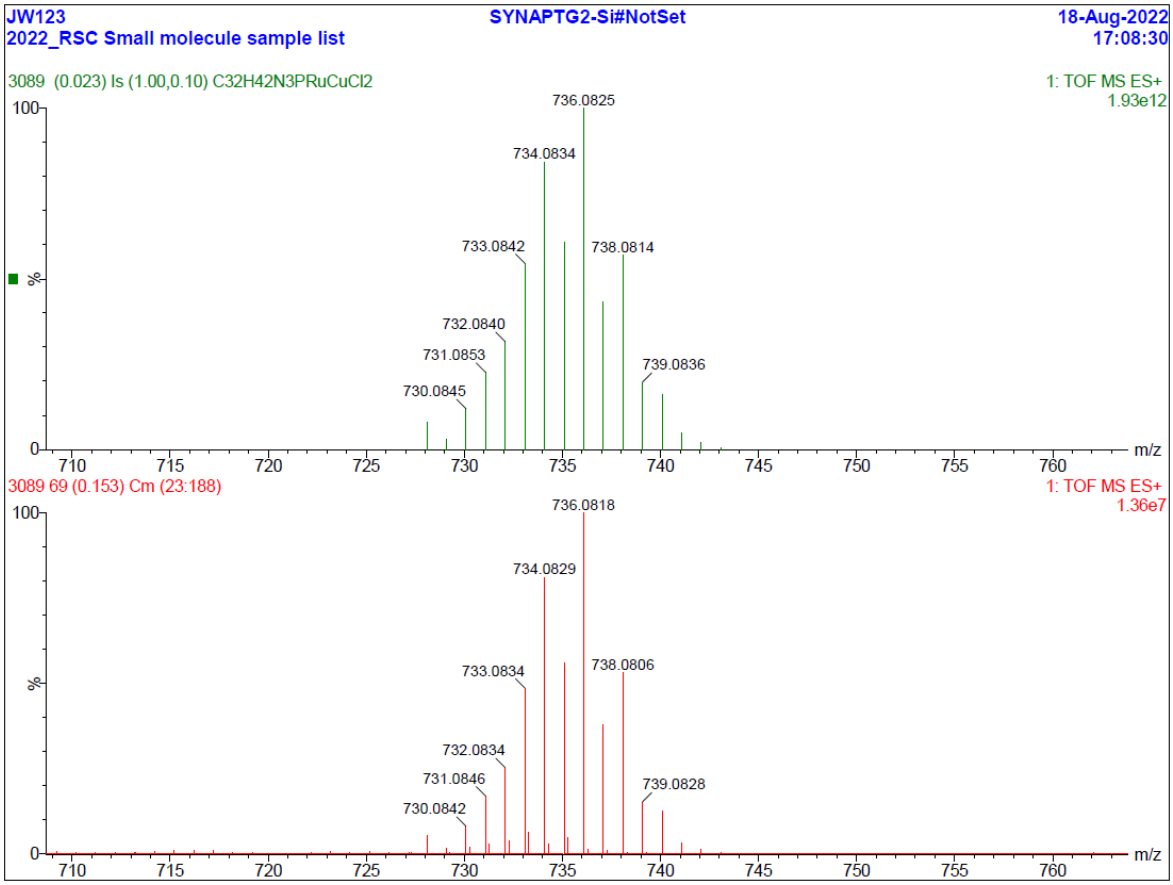

Figure S35. Experimental (bottom) and simulated (top) high resolution mass spectra (ESI+) of [$RuCuCl_3$(cymene)(PNNN)] (**3**).

6. Characterisation data for $[RuCuCl_2(cymene)(PNNN)]_2[PF_6]_2$ ($[\mathbf{4}]_2[\mathbf{PF_6}]_2$)

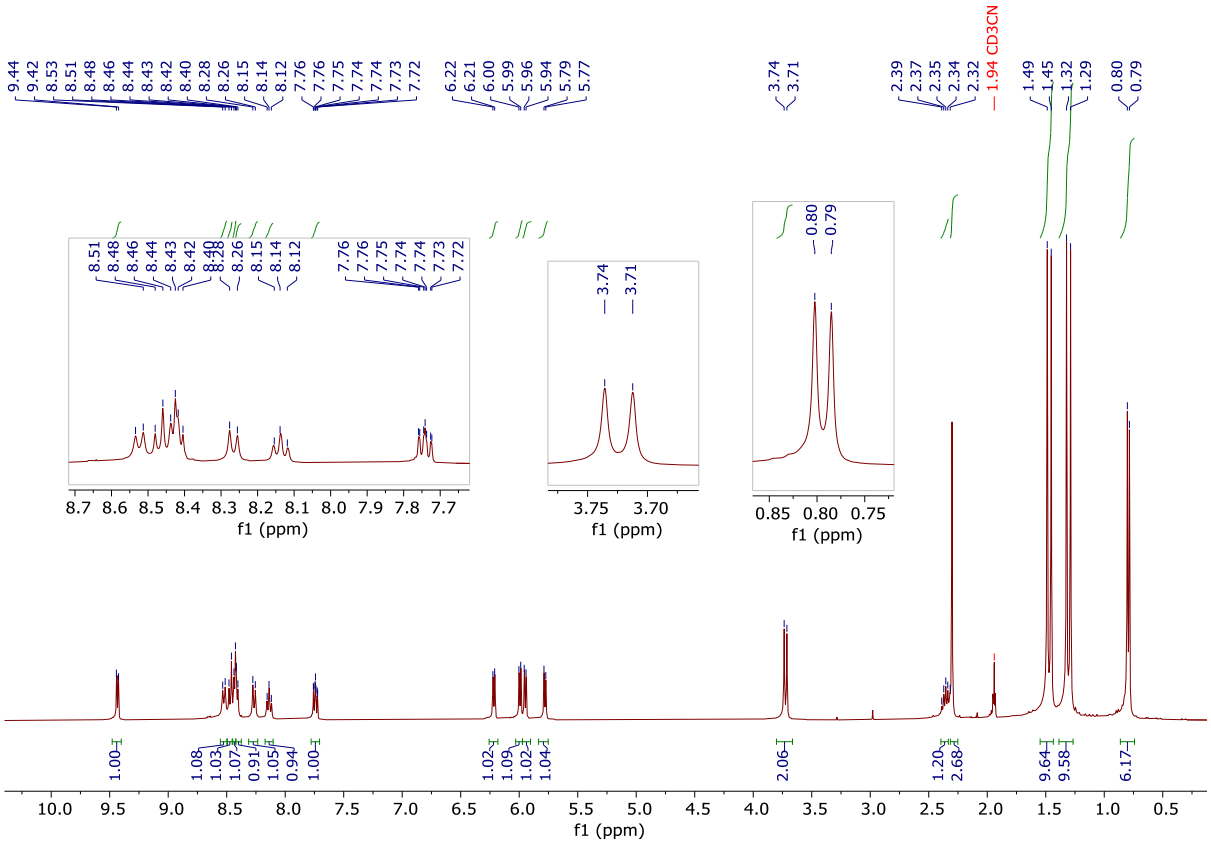

Figure S36. ^{1}H NMR spectrum of $[RuCuCl_2(cymene)(PNNN)]_2[PF_6]_2$ ($[\mathbf{4}]_2[\mathbf{PF_6}]_2$) (400 MHz, CD_3CN, 298 K).

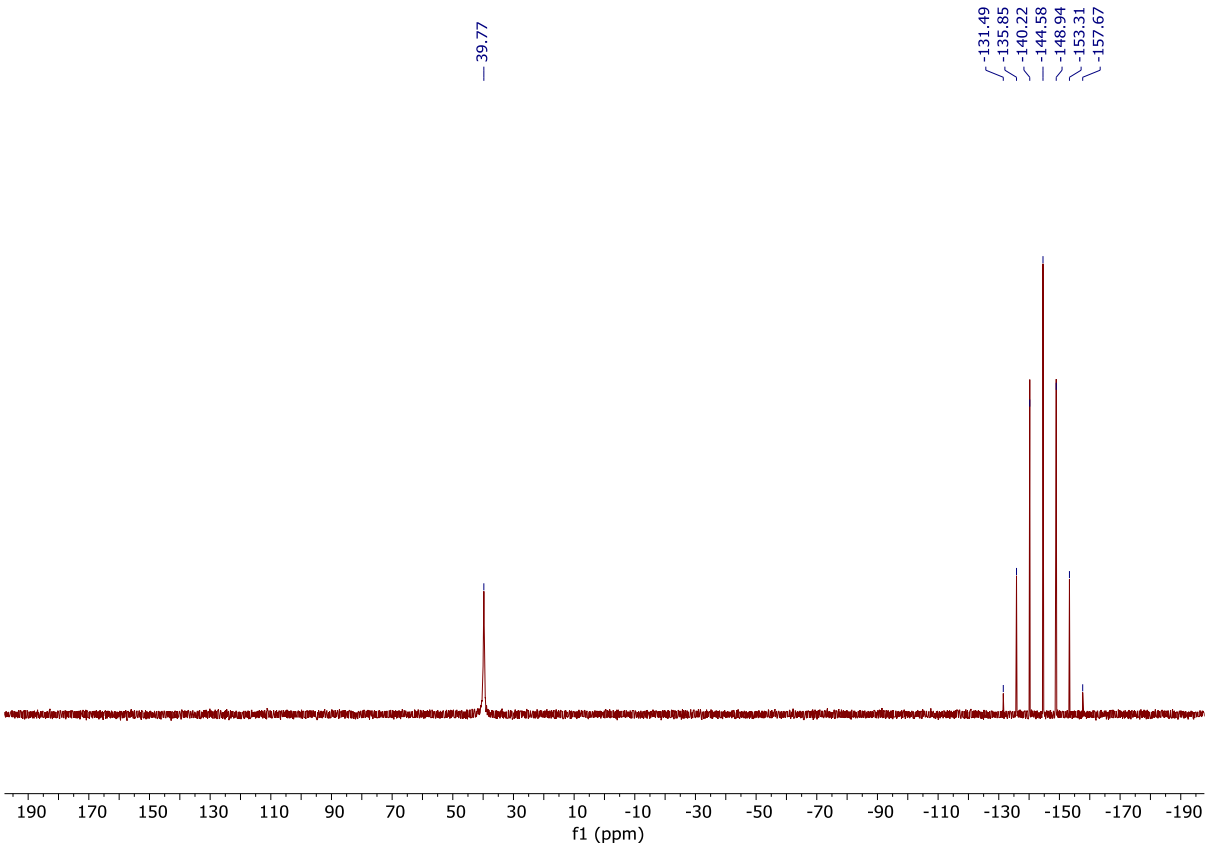

Figure S37. $^{31}P\{^1H\}$ NMR spectrum of $[RuCuCl_2(cymene)(PNNN)]_2[PF_6]_2$ ($[\mathbf{4}]_2[\mathbf{PF_6}]_2$) (162 MHz, CD_3CN, 298 K).

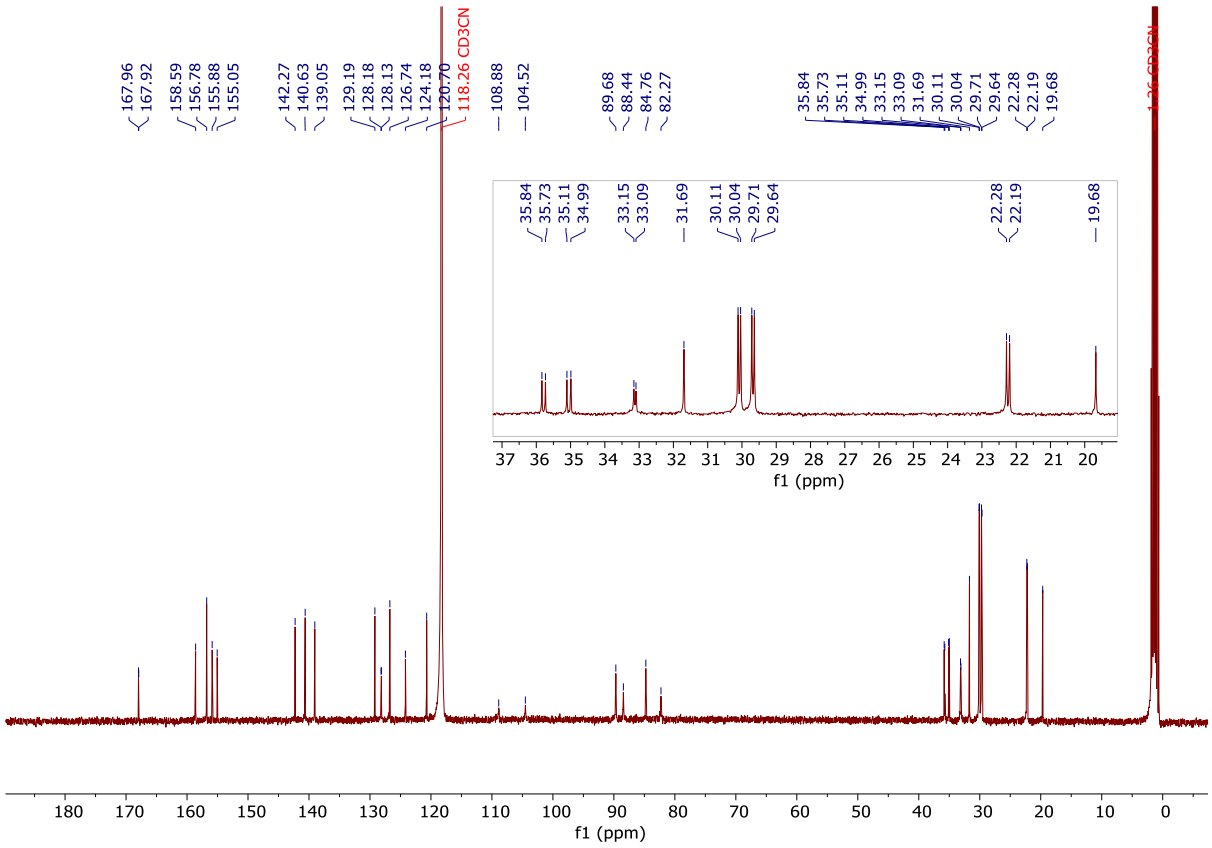

Figure S38. $^{13}C\{^{1}H\}$ NMR spectrum of $[RuCuCl_2(cymene)(PNNN)]_2[PF_6]_2$ (**[4]$_2$[PF$_6$]$_2$**) (101 MHz, CD_3CN, 298 K).

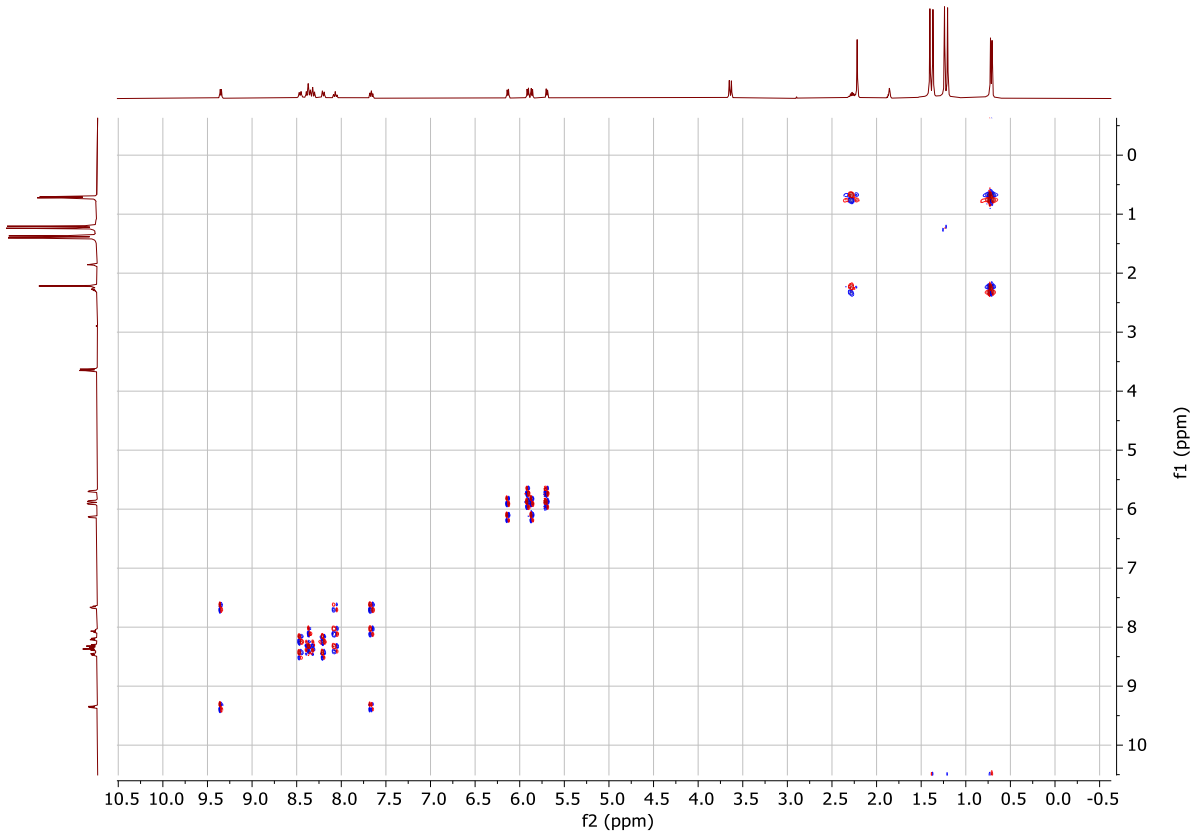

Figure S39. ^{1}H-^{1}H COSY NMR spectrum of $[RuCuCl_2(cymene)(PNNN)]_2[PF_6]_2$ (**[4]$_2$[PF$_6$]$_2$**) (400 MHz, CD_3CN, 298 K).

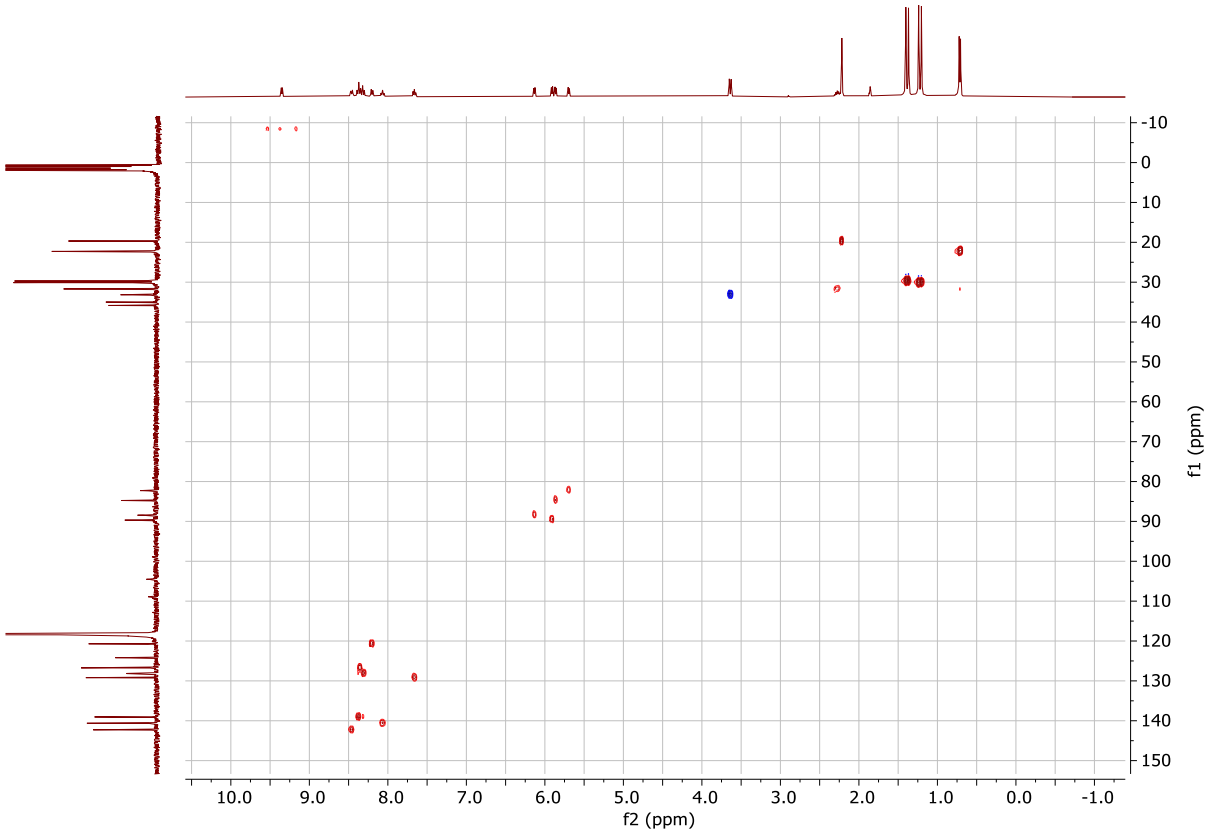

Figure S40. ^{1}H-^{13}C HSQC NMR spectrum of $[RuCuCl_2(cymene)(PNNN)]_2[PF_6]_2$ (**[4]$_2$[PF$_6$]$_2$**) (101, 400 MHz, CD_3CN, 298 K).

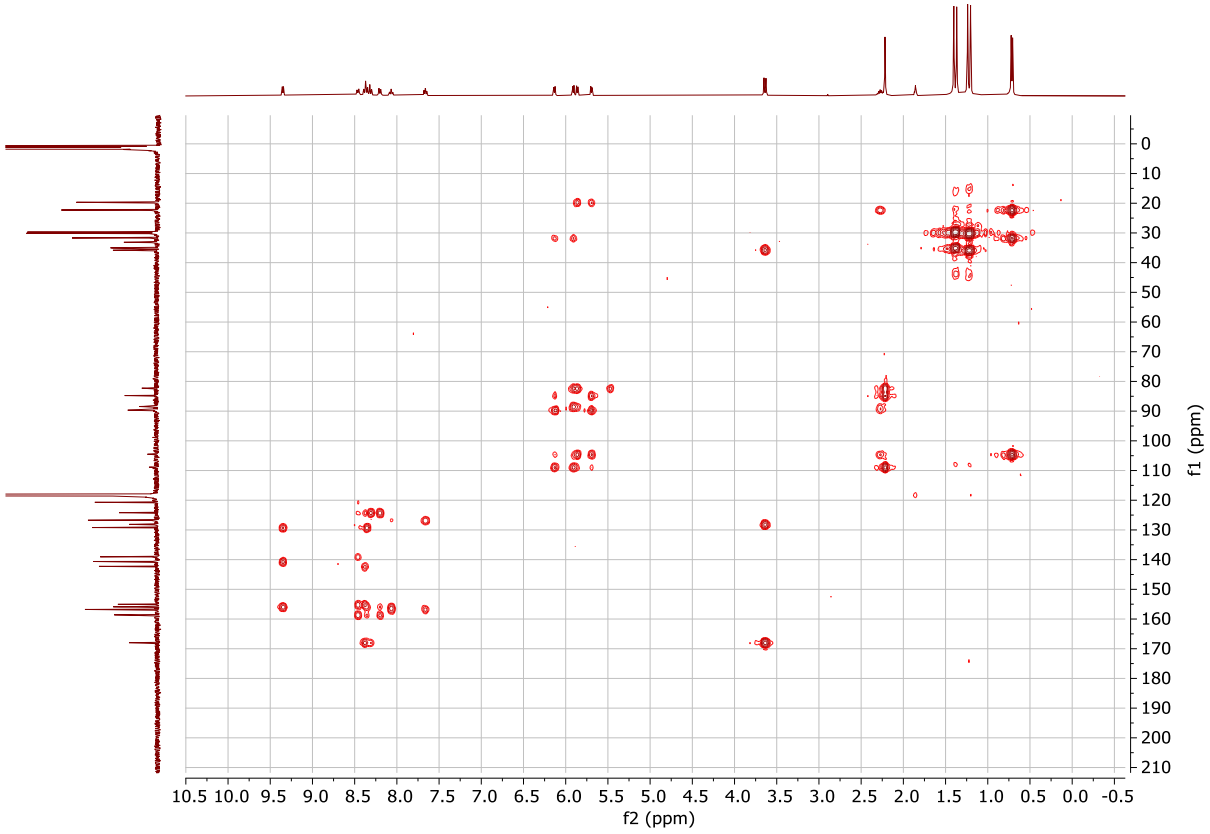

Figure S41. ^{1}H-^{13}C HMBC NMR spectrum of $[RuCuCl_2(cymene)(PNNN)]_2[PF_6]_2$ (**[4]$_2$[PF$_6$]$_2$**) (101, 400 MHz, CD_3CN, 298 K).

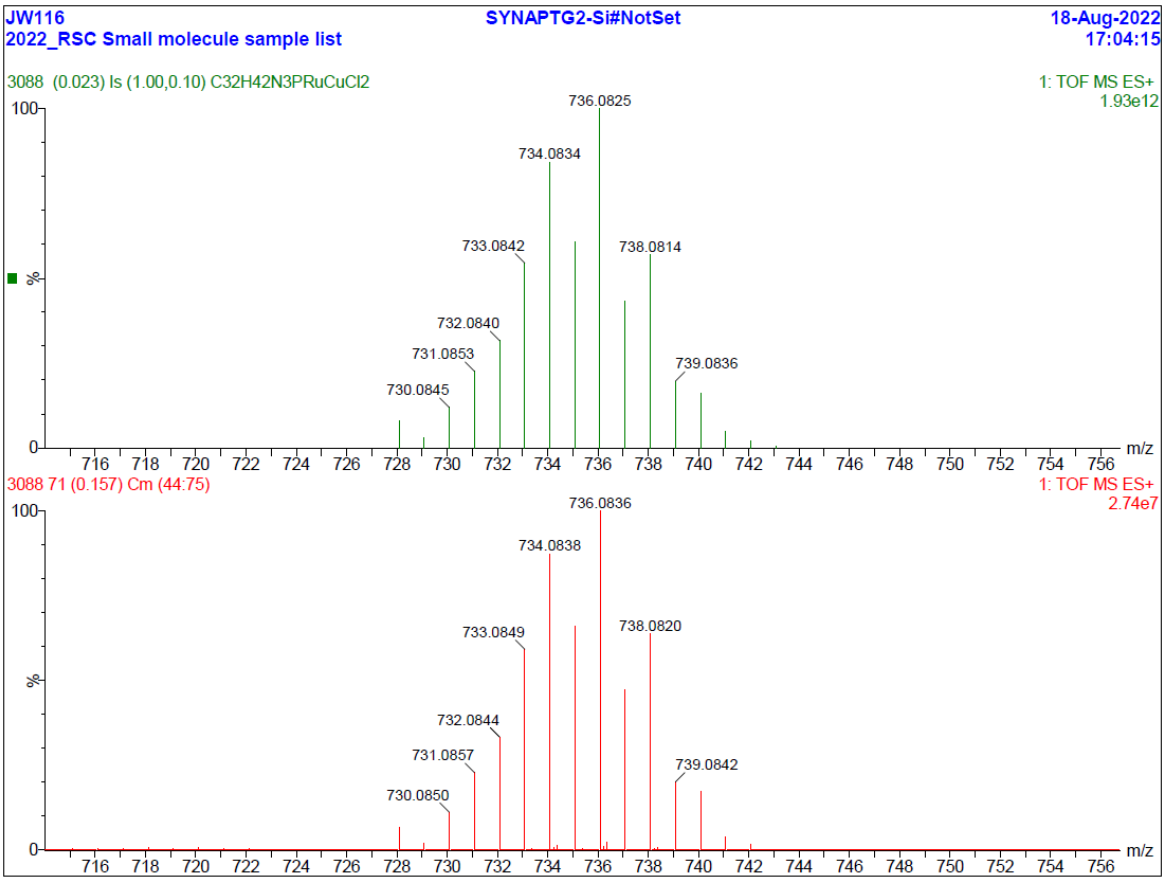

Figure S42. Experimental (bottom) and simulated (top) high resolution mass spectra (ESI+) of $[RuCuCl_2(cymene)(PNNN)]_2[PF_6]_2$ (**$[4]_2[PF_6]_2$**).

7. Characterisation data for [$Cu_2(O^tBu)(PNNN^*)$] (5)

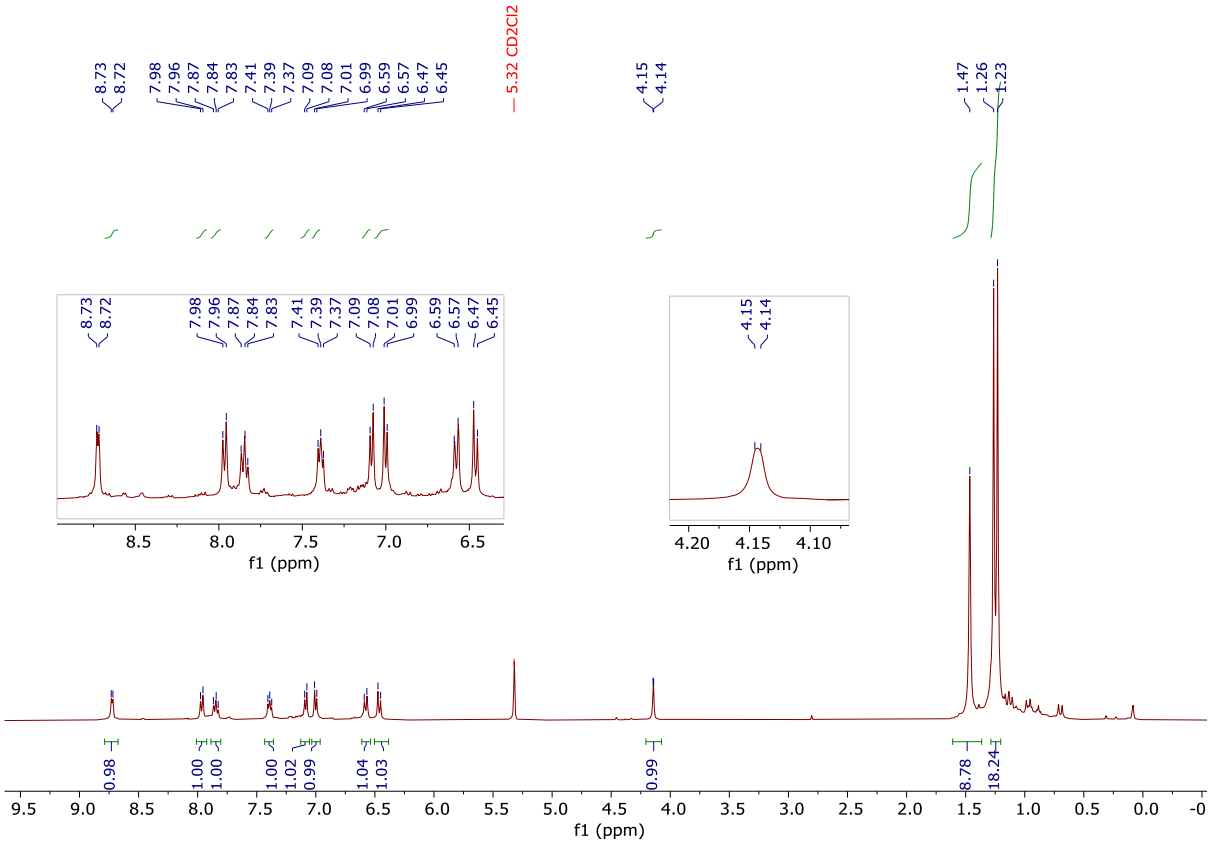

Figure S43. ^{1}H NMR spectrum of [$Cu_2(O^tBu)(PNNN^*)$] (**5**) (400 MHz, CD_2Cl_2, 298 K).

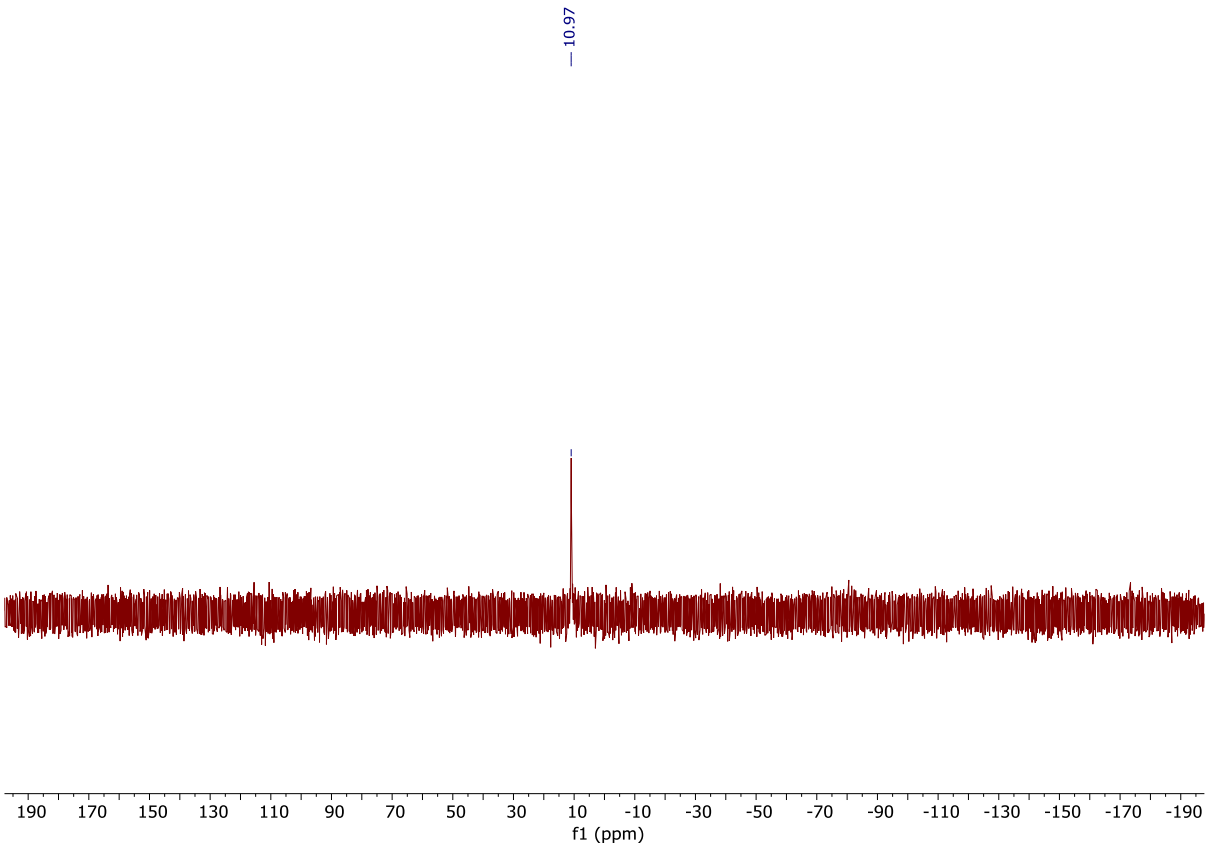

Figure S44. $^{31}P\{^1H\}$ NMR spectrum of [$Cu_2(O^tBu)(PNNN^*)$] (**5**) (162 MHz, CD_2Cl_2, 298 K).

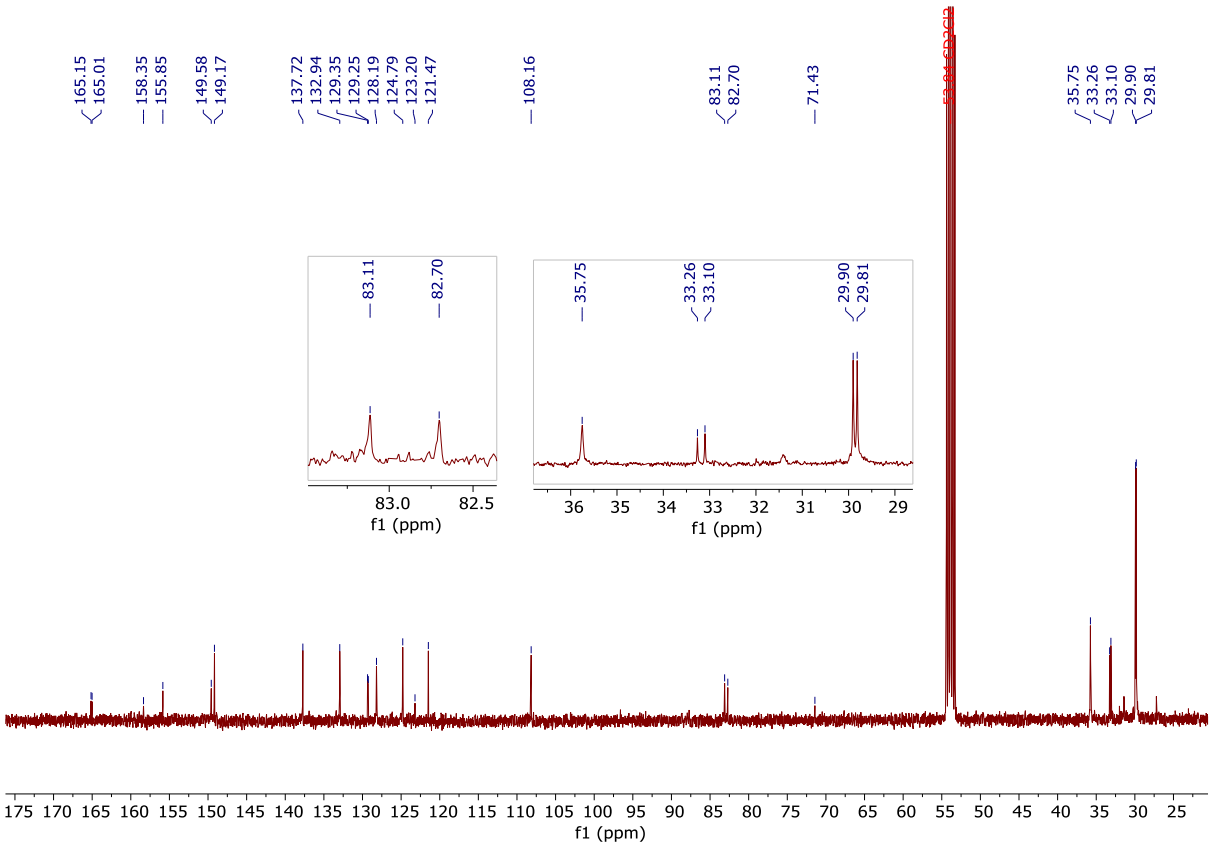

Figure S45. $^{13}C\{^{1}H\}$ NMR spectrum of $[Cu_2(O^tBu)(PNNN^*)]$ (**5**) (101 MHz, CD_2Cl_2, 298 K).

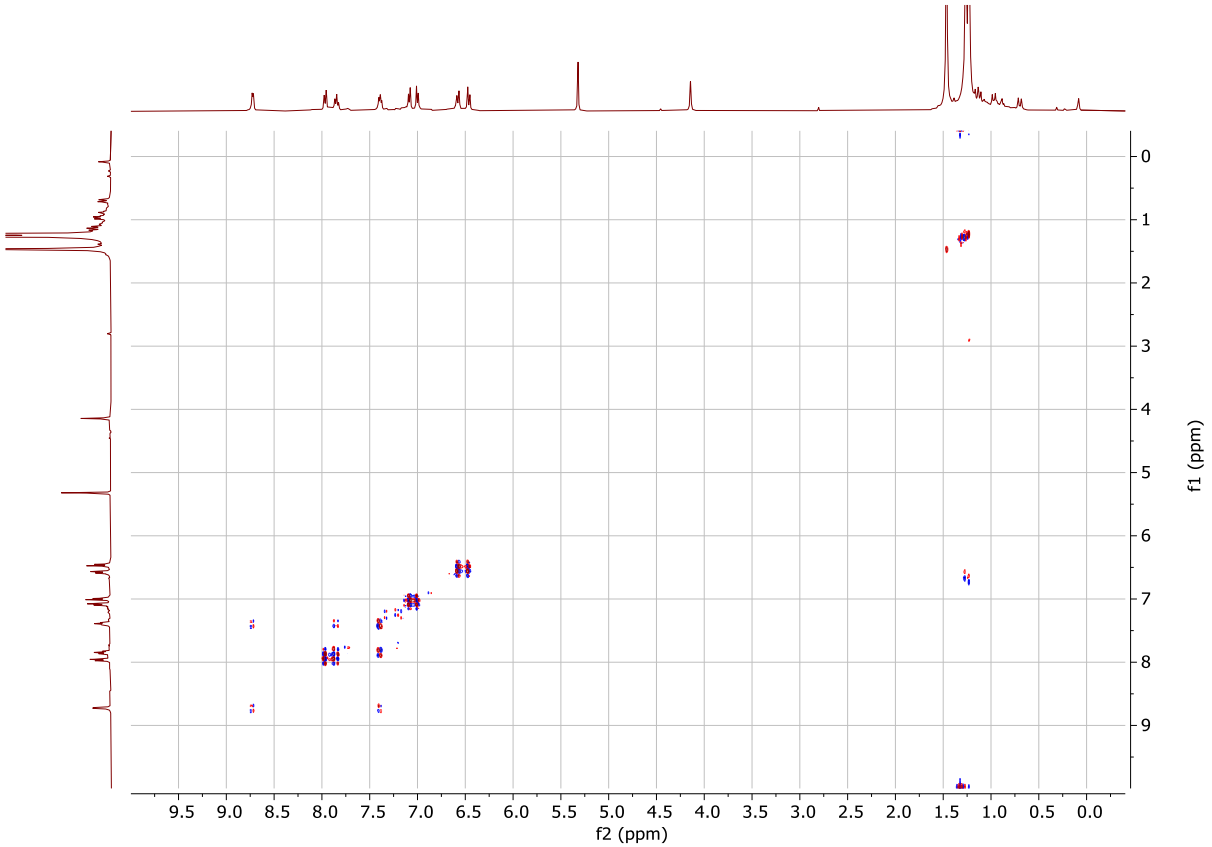

Figure S46. ^{1}H-^{1}H COSY NMR spectrum of $[Cu_2(O^tBu)(PNNN^*)]$ (**5**) (400 MHz, CD_2Cl_2, 298 K).

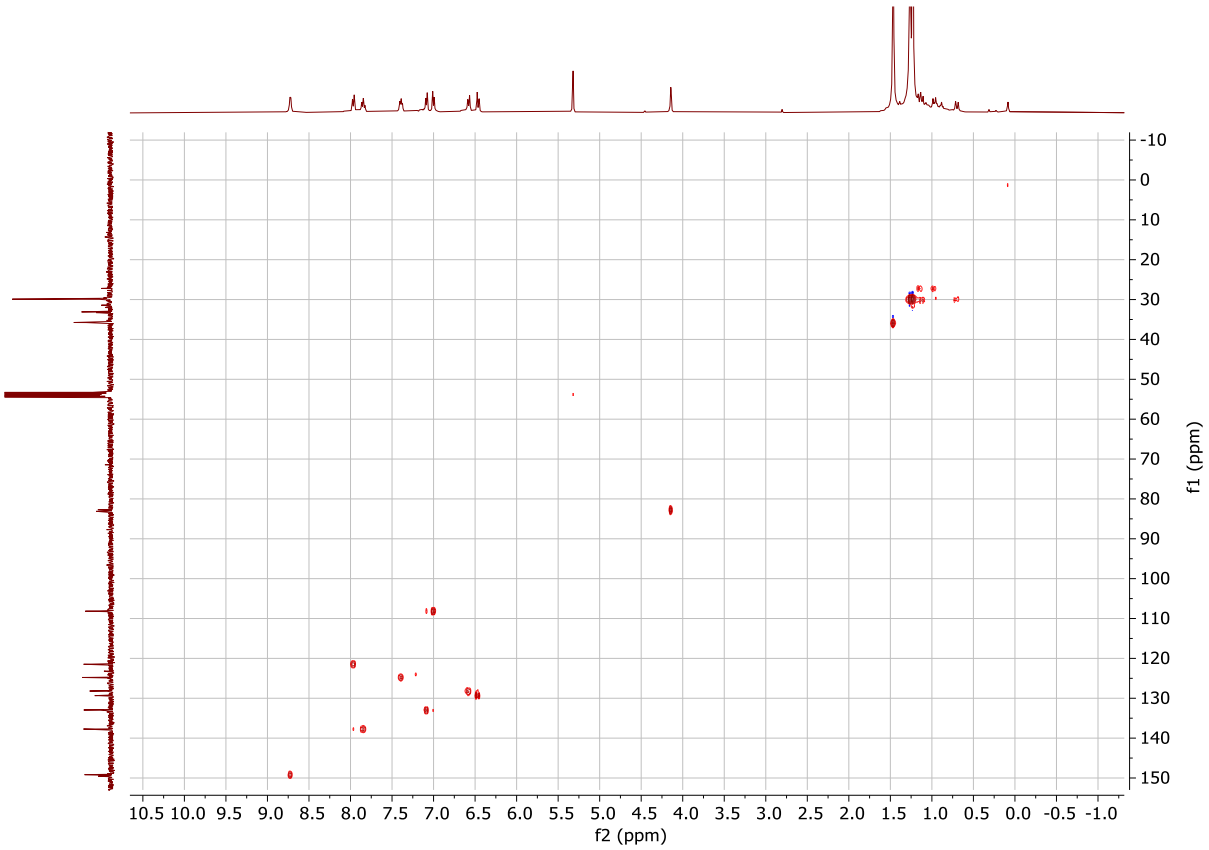

Figure S47. ^{1}H-^{13}C HSQC NMR spectrum of $[Cu_2(O^tBu)(PNNN^*)]$ (**5**) (101, 400 MHz, CD_2Cl_2, 298 K).

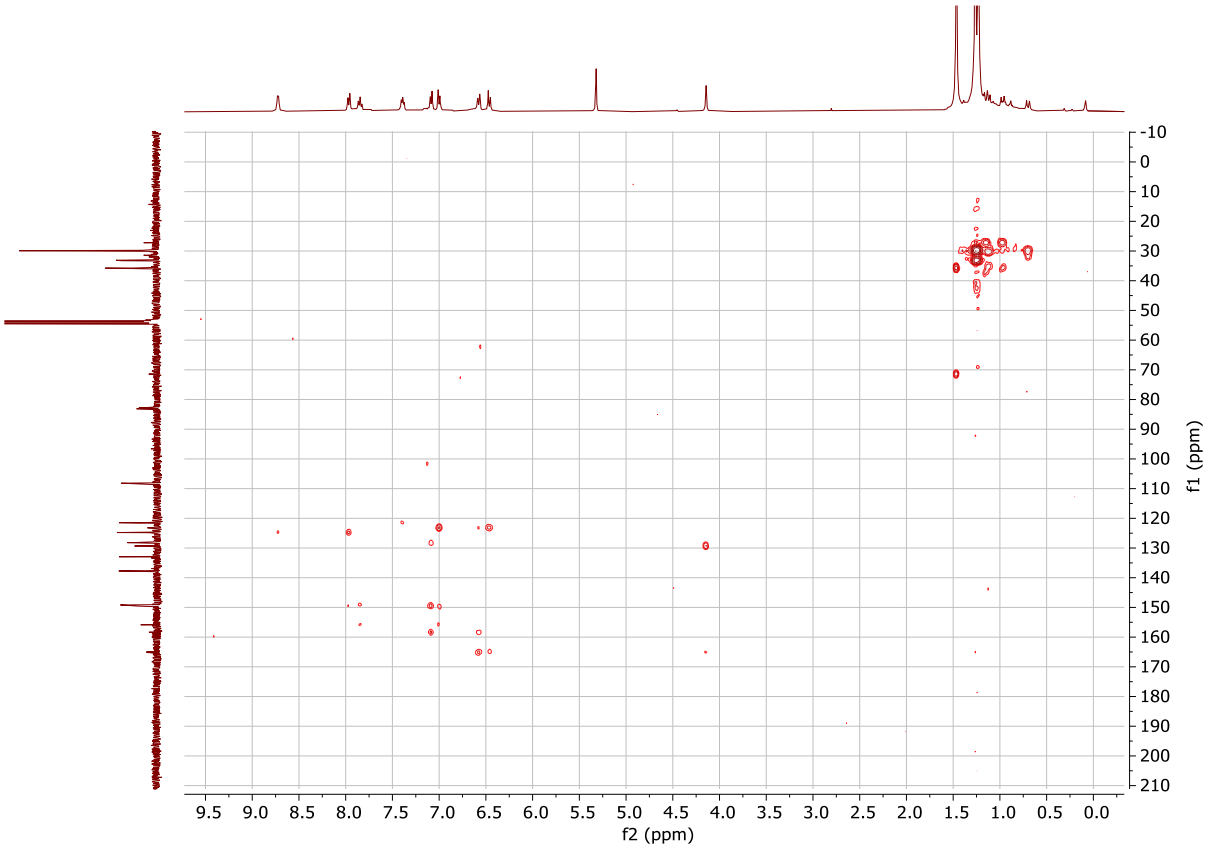

Figure S48. ^{1}H-^{13}C HMBC NMR spectrum of $[Cu_2(O^tBu)(PNNN^*)]$ (**5**) (101, 400 MHz, CD_2Cl_2, 298 K).

8. Characterisation data for [RuCuCl(cymene)(PNNN*)]PF_6 ([6]PF_6)

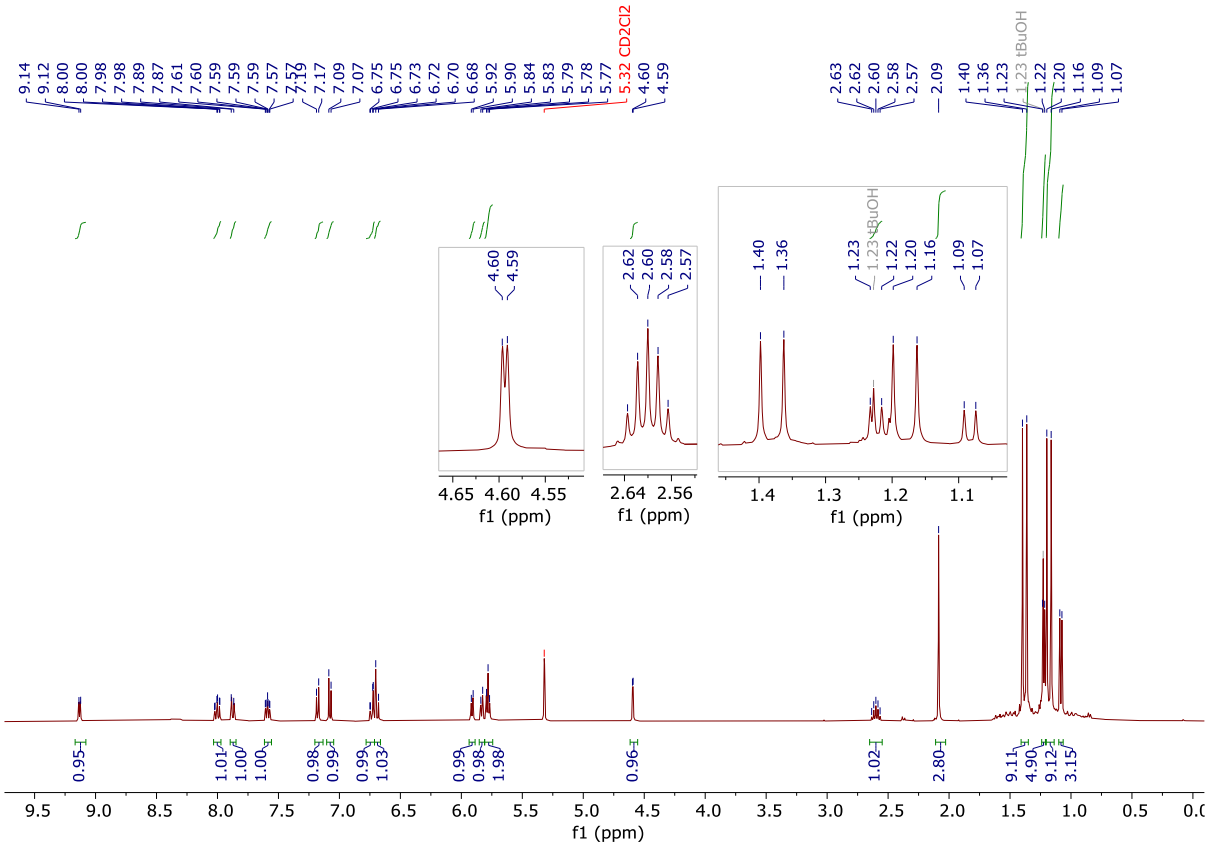

Figure S49. ^{1}H NMR spectrum of [RuCuCl(cymene)(PNNN*)]PF_6 (**[6]PF_6**) (400 MHz, CD_2Cl_2, 298 K).

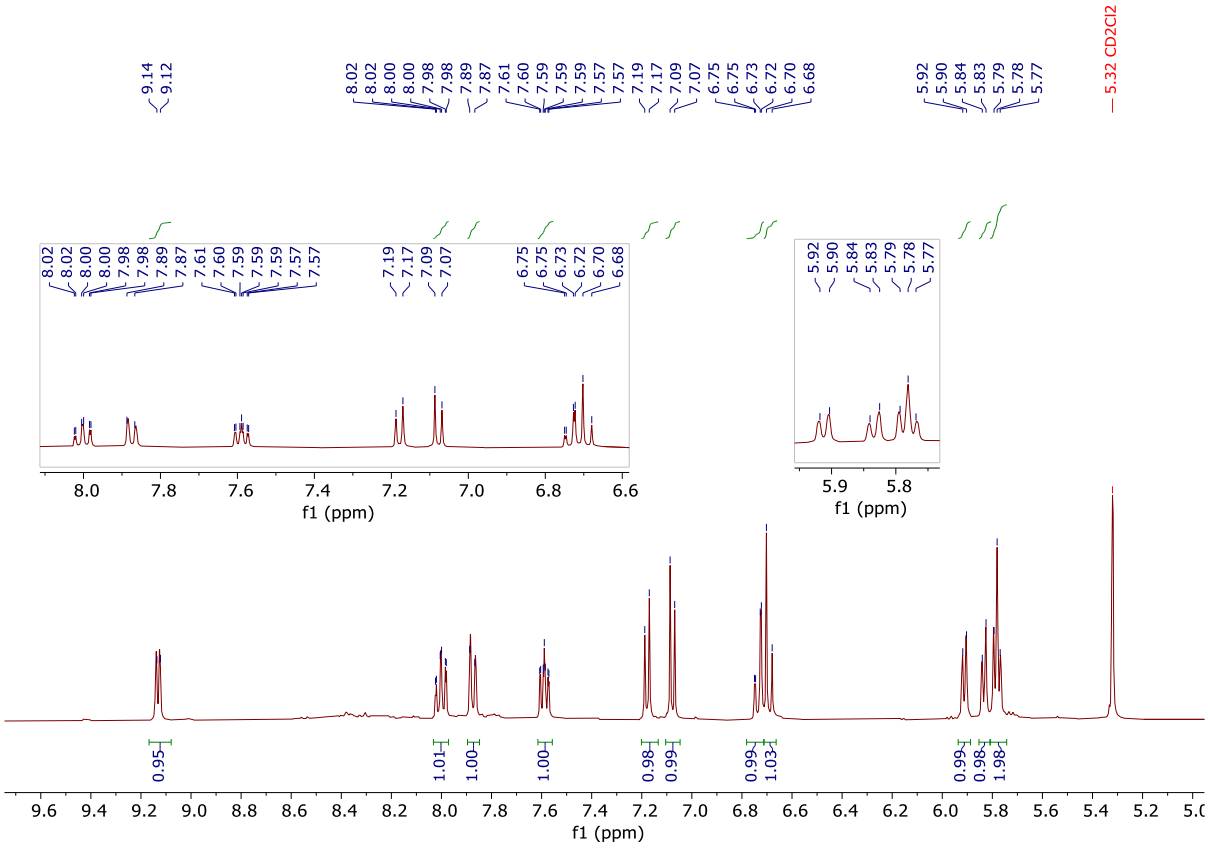

Figure S50. Aromatic region of the ^{1}H NMR spectrum of [RuCuCl(cymene)(PNNN*)]PF_6 (**[6]PF_6**) (400 MHz, CD_2Cl_2, 298 K).

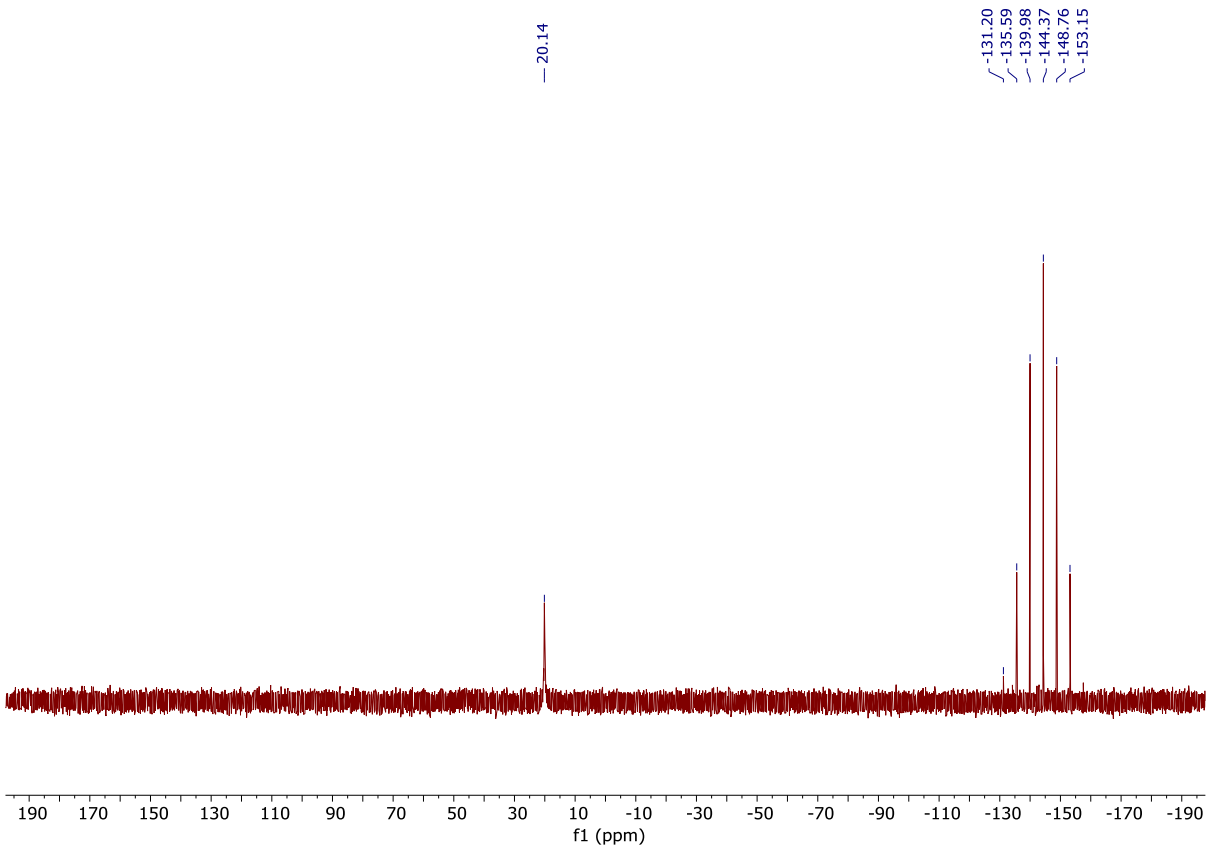

Figure S51. $^{31}P\{^{1}H\}$ NMR spectrum of [RuCuCl(cymene)(PNNN*)]PF_6 (**[6]PF_6**) (162 MHz, CD_2Cl_2, 298 K).

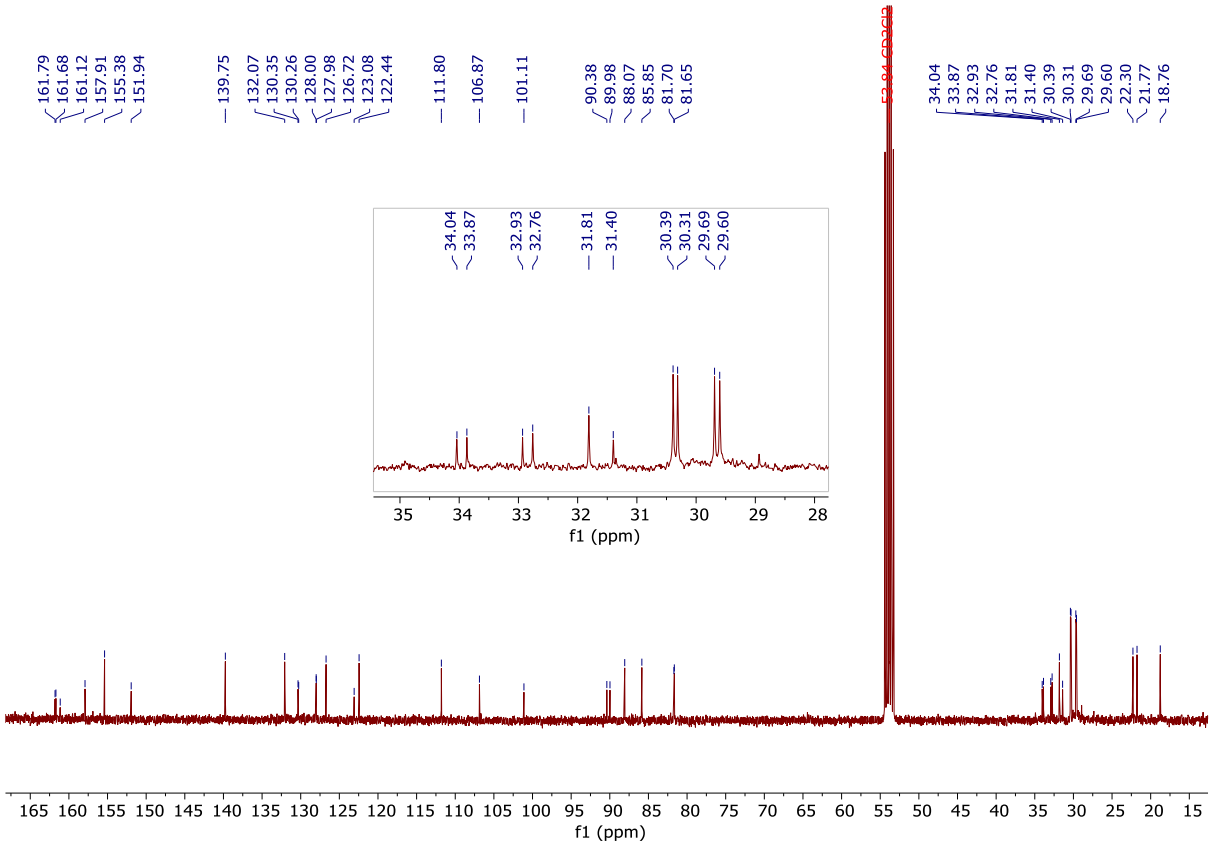

Figure S52. $^{13}C\{^{1}H\}$ NMR spectrum of [RuCuCl(cymene)(PNNN*)]PF_6 (**[6]PF_6**) (101 MHz, CD_2Cl_2, 298 K).

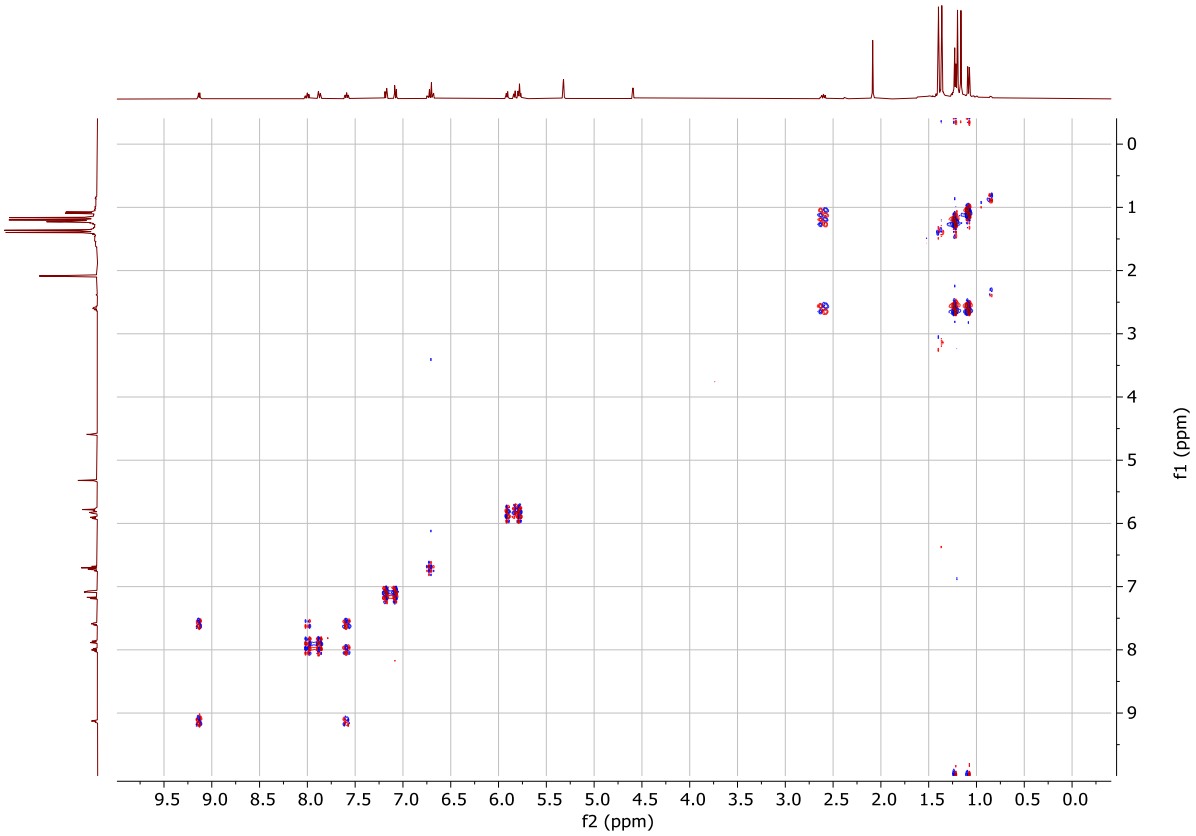

Figure S53. ^{1}H-^{1}H COSY NMR spectrum of [RuCuCl(cymene)(PNNN*)]PF_6 (**[6]PF_6**) (400 MHz, CD_2Cl_2, 298 K).

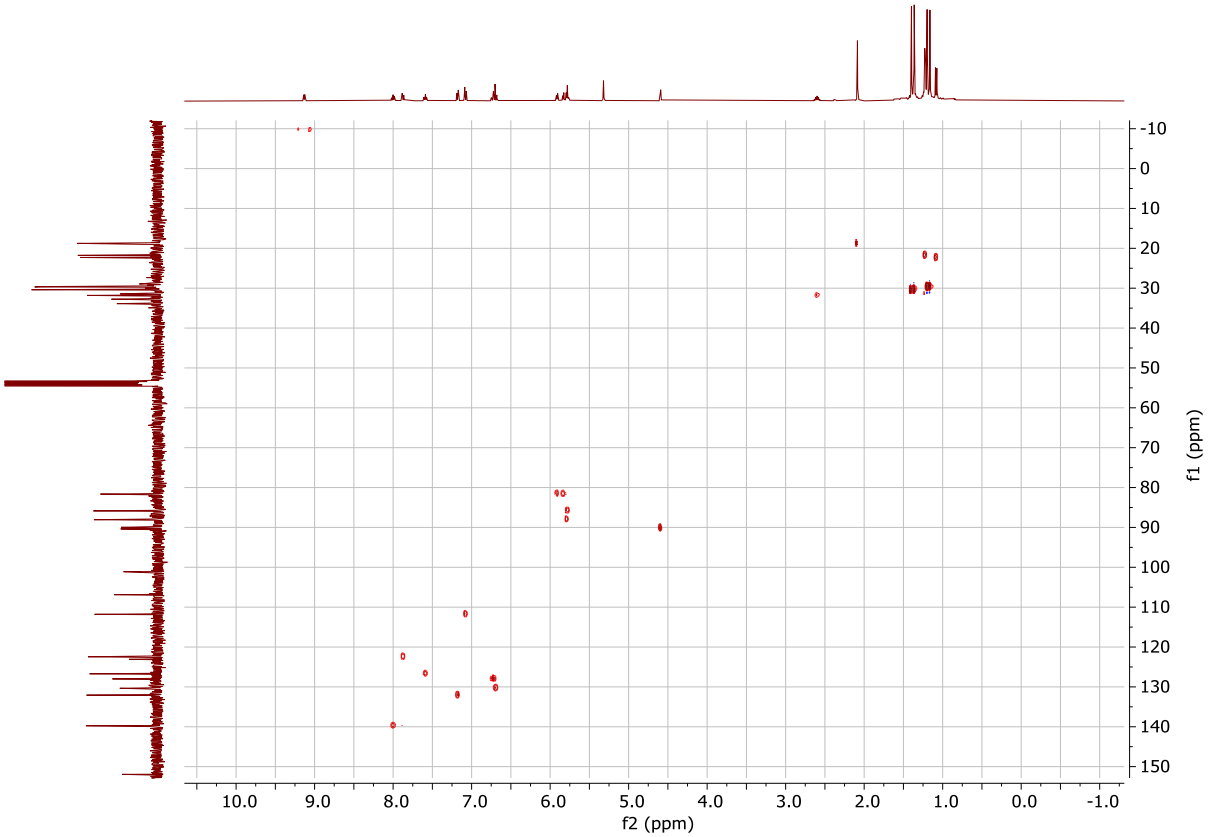

Figure S54. ^{1}H-^{13}C HSQC NMR spectrum of [RuCuCl(cymene)(PNNN*)]PF_6 (**[6]PF_6**) (101, 400 MHz, CD_2Cl_2, 298 K).

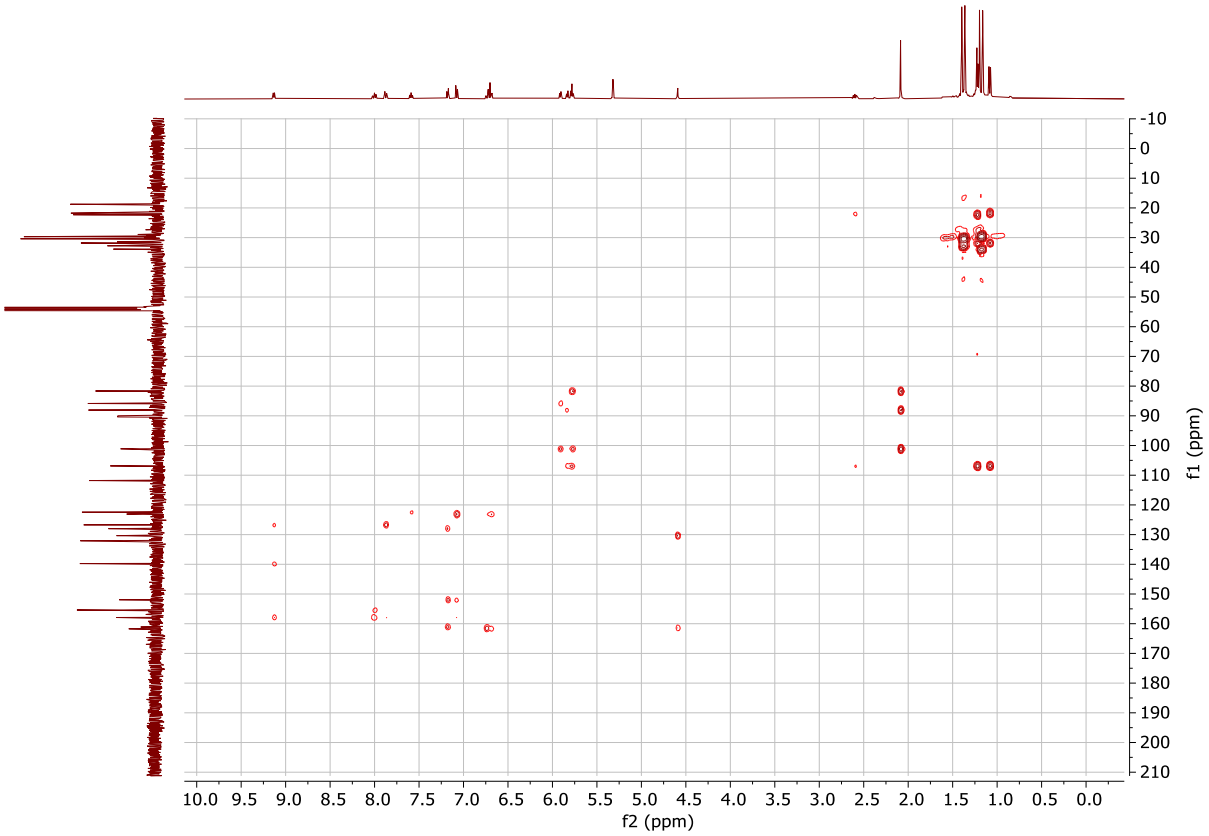

Figure S55. ^{1}H-^{13}C HMBC NMR spectrum of [RuCuCl(cymene)(PNNN*)]PF_6 (**[6]PF_6**) (101, 400 MHz, CD_2Cl_2, 298 K).

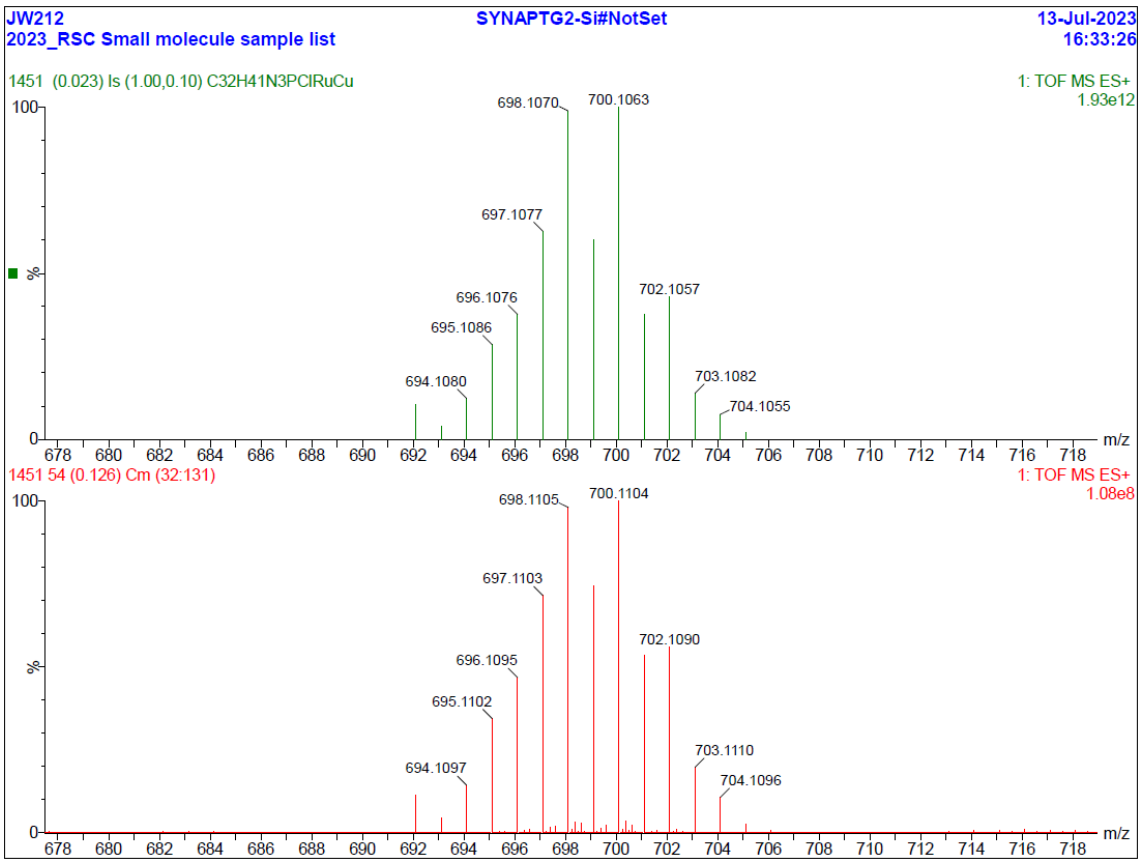

Figure S56. Experimental (bottom) and simulated (top) high resolution mass spectra (ESI+) of [RuCuCl(cymene)(PNNN*)]PF_6 (**[6]PF_6**).

9. X-ray crystallographic data

Table S1. X-ray crystallographic data for reported compounds.

Compound	$(PNNN)_2 \cdot CHCl_3$	$[Cu_2Cl_2(PNNN)] \cdot CH_2Cl_2$ (**1**$\cdot CH_2Cl_2$)	[RuCl(cymene)(PNNN)] Cl (**[2]Cl**)	$[RuCuCl_3(cymene)(PNNN)] \cdot (MeCN)_2$ (**3**$\cdot (MeCN)_2$)	$[RuCuCl_2(cymene)(PNNN)]_2 [PF_6]_{1.655}[CuCl_2]_{0.345} \cdot (MeCN)_2$ (**$[4]_2[PF_6]_{1.655}[CuCl_2]_{0.345} \cdot (MeCN)_2$**)	$[Cu_2(OtBu)(PNNN^*)]$ (**5**)	$[RuCuCl(cymene)(PNNN^*)] PF_6$ (**$[6]PF_6$**)
CCDC number	2386871	2386871	2386872	2386873	2386874	2386875	2386876
Chemical formula	$2(C_{22}H_{28}N_3P)$, $CHCl_3$	$C_{22}H_{28}Cl_2Cu_2N_3P$ CH_2Cl_2	$C_{32}H_{43}Cl_2N_3PRu$	$C_{32}H_{42}Cl_3CuN_3PRu$, $2(C_2H_3N)$	$C_{64}H_{84}Cl_4Cu_2N_6P_2Ru_2$, $1.655(F_6P)$, $0.345(Cl_2Cu)$, $2(C_2H_3N)$	$C_{26}H_{36}Cu_2N_3OP$	$C_{32}H_{41}ClCuN_3PRu$, F_6P
Formula weight	850.25	648.35	636.1854	736.0825	1838.77	564.63	843.68
Temperature/K	150.00(10)	150.00(10)	150.00(10)	150.00(10)	150.00(10)	150.00(10)	100(2)
Crystal system	Monoclinic	Triclinic	Tetragonal	Triclinic	Triclinic	Triclinic	Triclinic
Space group	$P2_1$	*P-1*	$I4_1/a$	*P-1*	*P-1*	*P-1*	*P-1*
a/Å	18.4963(2)	9.7176(3)	32.5802(3)	11.0189(2)	8.3879(3)	8.2661(3)	8.3590(17)
b/Å	6.17950(10)	13.0045(5)	32.5802(3)	12.5547(2)	16.3160(6)	11.0365(3)	10.554(2)
c/Å	20.5648(3)	13.0393(3)	12.6410(3)	14.1481(3)	16.3624(5)	15.4542(4)	20.422(4)
α/°	90	64.567(3)	90	87.736(2)	113.508(3)	96.178(2)	100.97(3)
β/°	107.9800(10)	68.136(3)	90	83.713(2)	100.048(3)	98.598(2)	97.18(3)
γ/°	90	75.453(3)	90	77.647(2)	96.419(3)	108.172(3)	93.89(3)
Volume/$Å^3$	2235.72(6)	1372.87(9)	13418.0(4)	1900.16(6)	1980.74(13)	1306.52(7)	1747.1(6)
Z	2	2	16	2	1	2	2
Radiation	Cu Kα	Cu Kα	Cu Kα	Cu Kα	Cu Kα	Cu Kα	Synchrotron – equivalent to Mo Kα
μ/mm^{-1}	2.827	6.175	5.877	1.54184	6.451	2.756	1.268
Dcalc/gcm^{-3}	1.263	1.568	1.332	1.490	1.541	1.435	1.604
Reflection measured	15589	14511	21093	22982	14037	7947	43947
Independent reflections	7852	5606	6925	7655	7822	5072	7496
R_{int}	0.0314	0.0402	0.0640	0.0238	0.0228	0.0194	0.0607
Final R_1 values [I > 2σ(I)]	0.0358	0.0476	0.0457	0.0277	0.0470	0.0341	0.0388
Final wR_2 values (all data)	0.0934	0.1241	0.1241	0.0697	0.1318	0.0938	0.1074
Goodness-of-fit on F^2	1.052	1.086	1.055	1.056	1.019	1.035	1.106

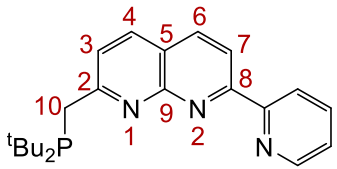

PNNN

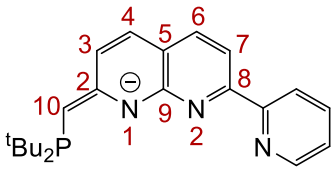

PNNN*

Figure S57. Atom numbering scheme used in Table S2.

Table S2. Comparison of PNNN vs PNNN* bond lengths from X-ray crystallographic analyses.

Bond	**Bond length (Å)**			
Compound	**[1]**	**[5]**	**$[4]_2[PF_6]_2$**	**$[6]PF_6$**
Ligand assignment	**PNNN**	**PNNN***	**PNNN**	**PNNN***
C2–C10	1.509(4)	1.376(3)	1.497(6)	1.360(4)
C2–C3	1.424(5)	1.449(3)	1.427(6)	1.458(4)
C3–C4	1.362(5)	1.338(3)	1.354(7)	1.334(5)
C4–C5	1.415(5)	1.436(3)	1.417(7)	1.435(5)
C5–C9	1.414(4)	1.429(3)	1.422(5)	1.439(4)
C5–C6	1.409(5)	1.387(3)	1.405(6)	1.375(5)
C6–C7	1.363(5)	1.379(4)	1.368(7)	1.387(5)
C7–C8	1.415(4)	1.381(3)	1.400(6)	1.388(4)
C2–N1	1.323(4)	1.388(3)	1.325(6)	1.402(4)
C9–N1	1.349(4)	1.356(3)	1.346(5)	1.333(4)
C8–N2	1.334(4)	1.346(3)	1.342(5)	1.360(4)
C9–N2	1.349(4)	1.357(3)	1.379(5)	1.371(4)